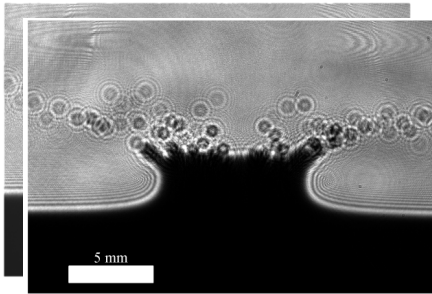*Exceptional service in the national interest*

Sandia National Laboratories
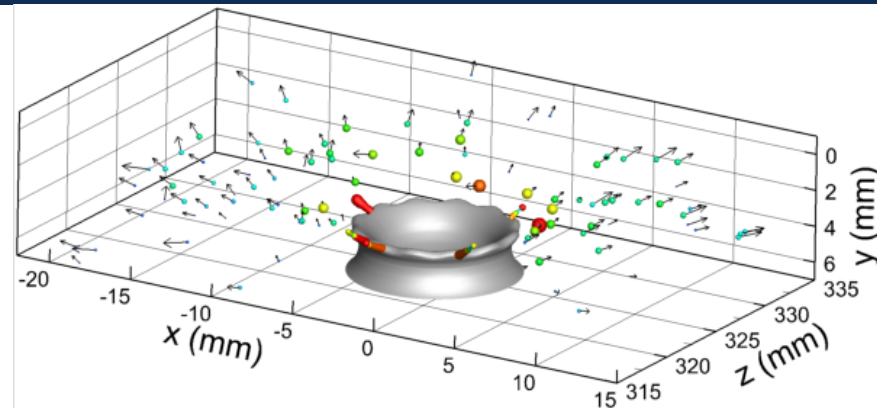
# Digital In-line Holography (DIH) for 3D Quantification of Inert and Reacting Particle Fields

Daniel R. Guildenbecher

August 12, 2015

Motivation: 3D imaging for a 3D world

Widely available 2D imaging or point-wise measurement techniques are often insufficient to resolve 3D flow phenomena

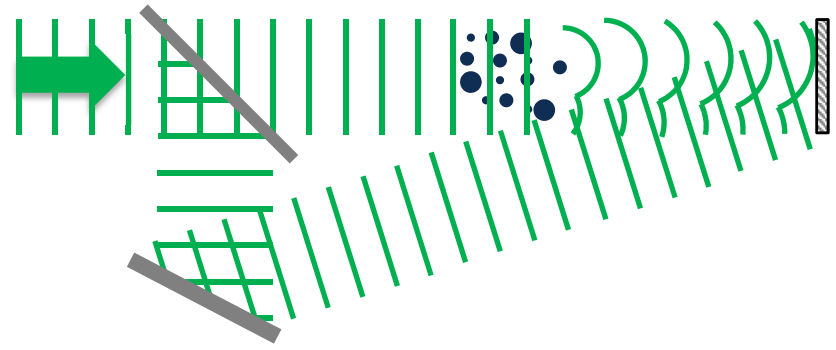- Repetition needed to capture spatial statistics

air flow

high-speed video of a ethanol drop in an air-stream
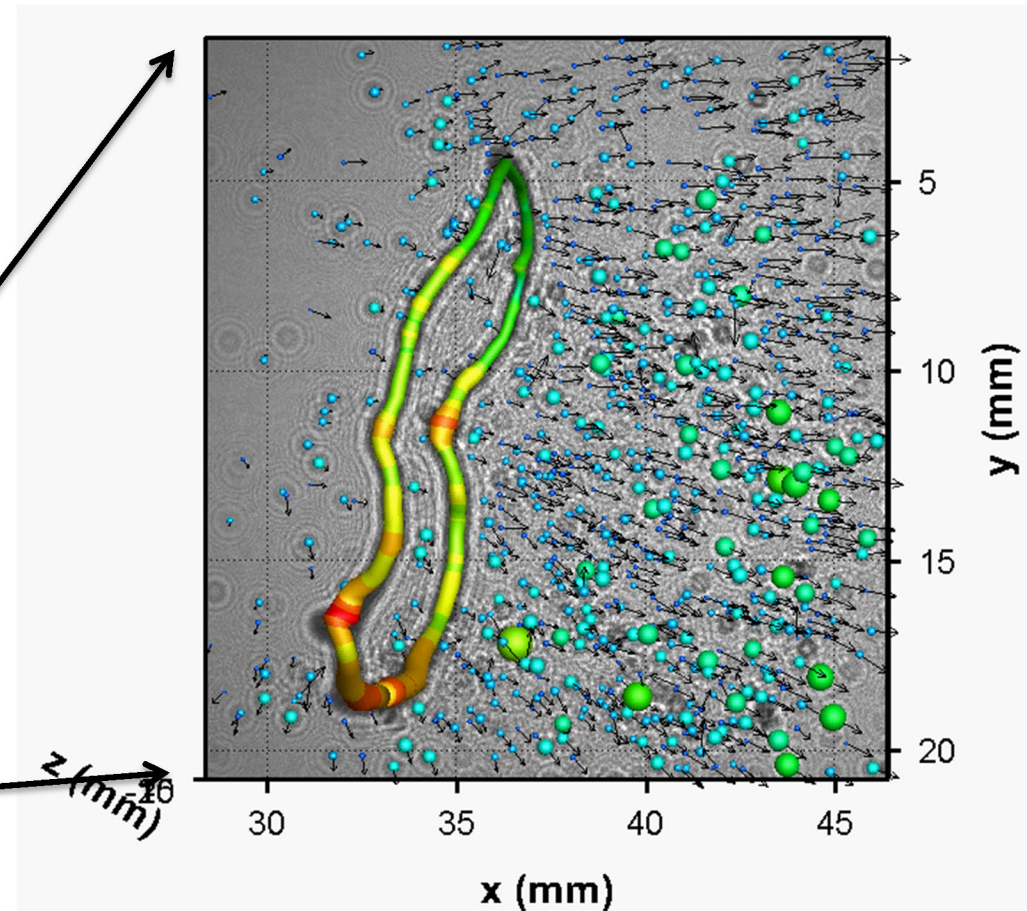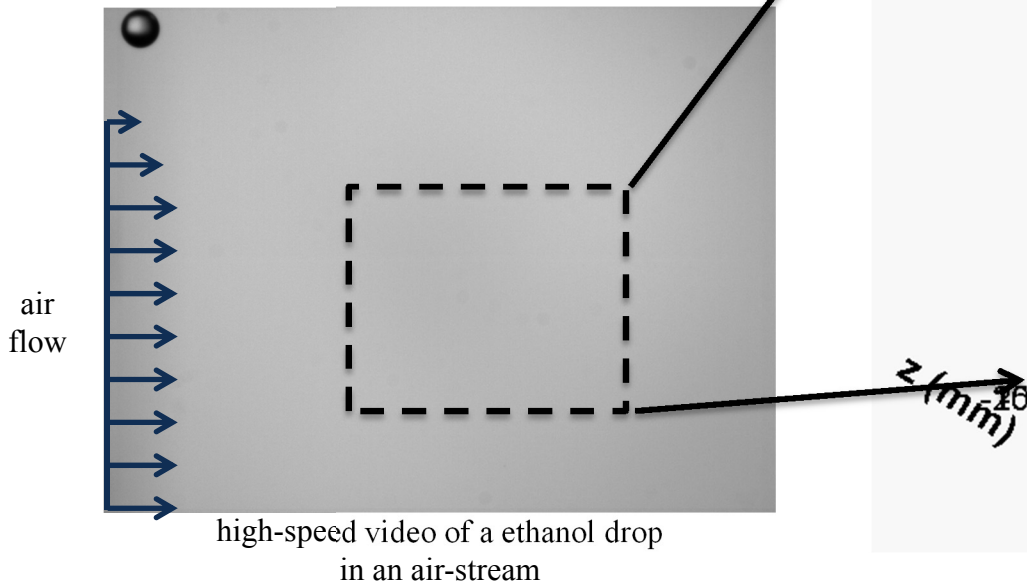
digital holographic measurement
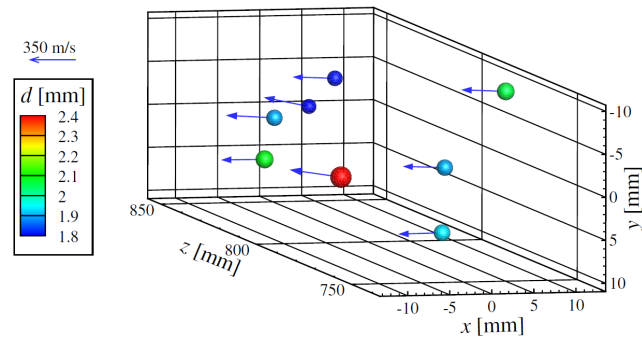(Gao, Guildenbecher et al, 2013, *Opt. Lett.*)

Holography is an optical technique to record and reconstruct a 3D light field
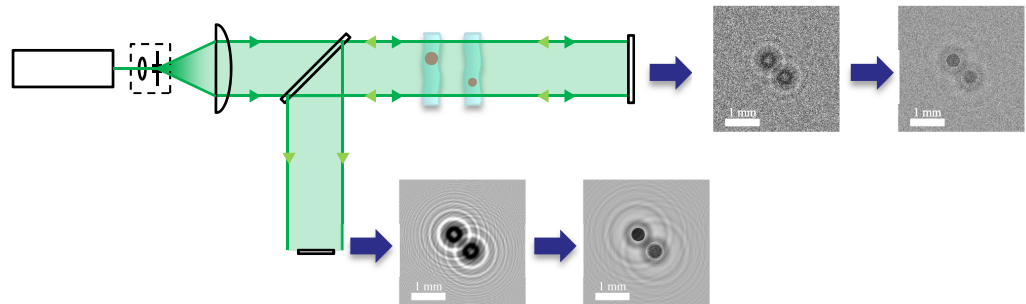
Outline for talk

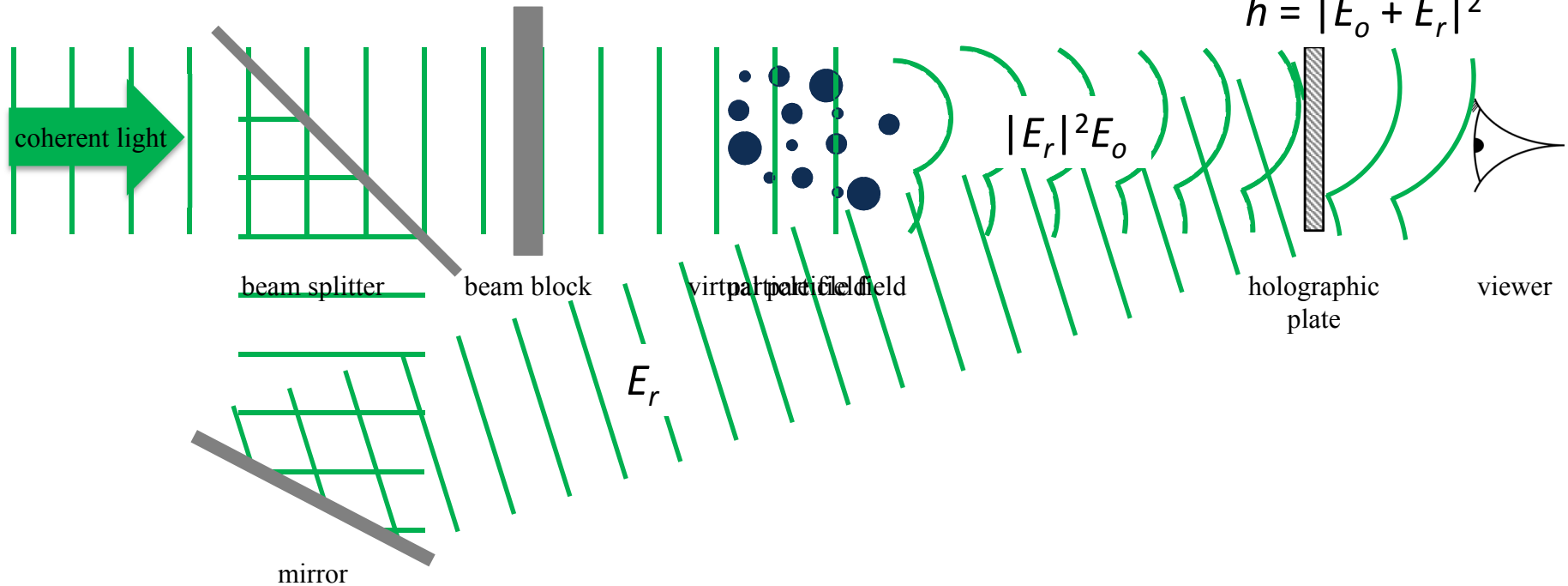Introduction to holography and the "digital revolution"

Particle measurements

New concepts and opportunities

What is holography?

Optical method first proposed by Gabor in 1948

1. Coherent light diffracted by particle field forms the object wave, E_o

2. Interference with a reference wave, E_r, forms the hologram: $h = |E_o + E_r|^2$

3. Reconstruction with E_r forms virtual images at original particle locations
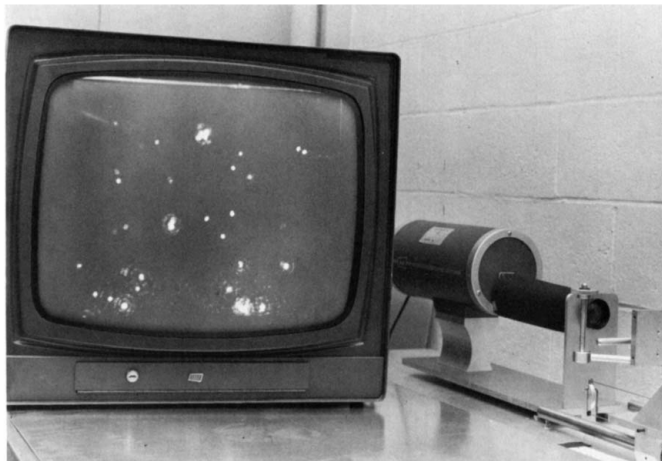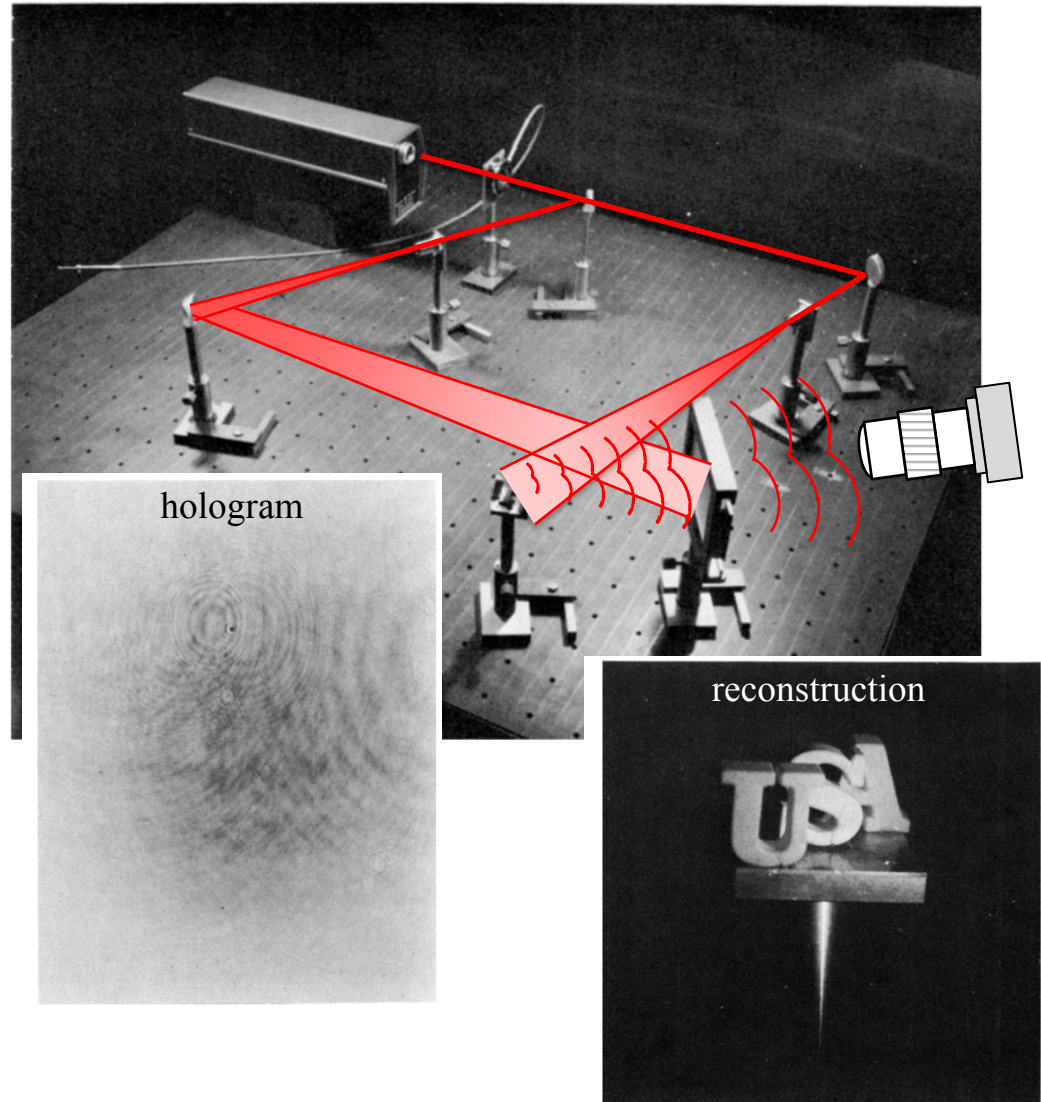
$$h \cdot E_r = \underbrace{(|E_o|^2 + |E_r|^2)E_r}_{\text{DC term}} + \underbrace{|E_r|^2 E_o}_{\substack{\text{virtual} \\ \text{image}}} + \underbrace{E_r^2 E_o^*}_{\substack{\text{real} \\ \text{image}}}$$

Analog holography

Applications of holography took off with invention of the laser in 1960

Challenges:

- Darkroom needed to process the hologram
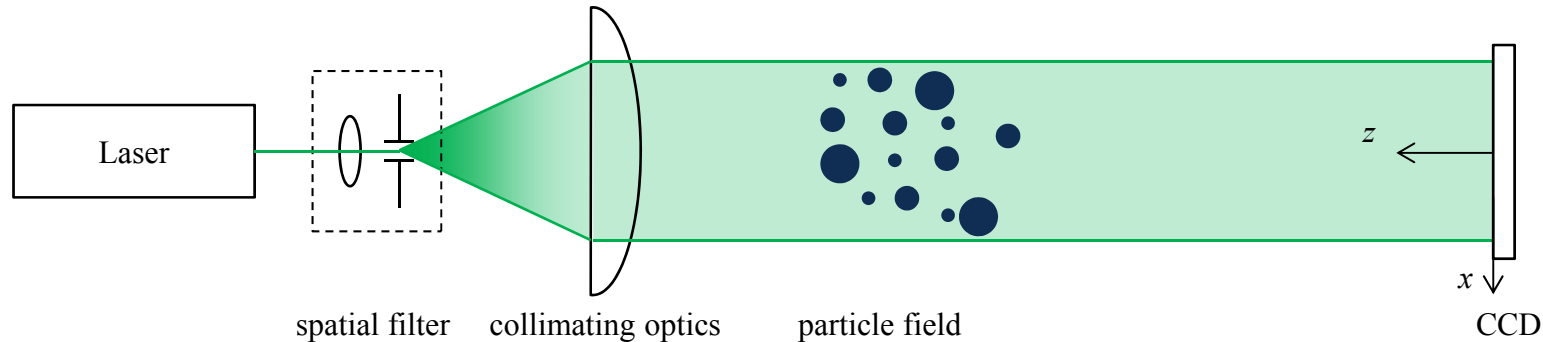
- Limited temporal resolution

- Manual post processing

hologram

reconstruction

Collier et al, 1971, *Optical Holography*

Thompson et al, 1967, *Appl. Opt.*

Digital in-line holography (DIH)

Holographic plate and wet-chemical processing replaced with digital sensor

- First proposed by Schnars and Jüptner in '90s

- <u>Advantages:</u> (1) no darkroom, (2) temporal resolution is straight forward, (3) results can be numerically refocused and post-processed

- <u>Challenge:</u> Resolution of digital sensors (order 100 line pairs/mm) is much less than resolution of photographic emulsions (order 5,000 line pairs/mm)

  - For suitable off axis angles, θ, the fringe frequency, f, is typically too large to resolve with digital sensors ($f = 2\sin(\theta/2)/\lambda$)
  - Rather, the in-line configuration ($\theta = 0$) is typically utilized

Numerical refocusing

Light propagation in a non-absorbing, constant index of refraction medium is described by the <u>diffraction integral equation</u>:

$$E(x,y,z) = \frac{1}{\lambda} \iint E(\xi,\eta,z=0) \frac{\exp\left[-jk\sqrt{(\xi-x)^2 + (\eta-y)^2 + z^2}\right]}{\sqrt{(\xi-x)^2 + (\eta-y)^2 + z^2}} \psi \, d\xi d\eta$$

- $E(\xi,\eta,0)$ ≡ complex amplitude at input plane
- $E(x,y,z)$ ≡ complex amplitude at output plane
- Mathematical expression of the Huygens-Fresnel principle

This convolution can solved in the frequency domain:

$$E(x,y,z) = \mathfrak{I}^{-1}\left[\mathfrak{I}[E(\xi,\eta,z=0)] \cdot G\left(f_x,f_y,z\right)\right]$$

- $\mathfrak{I}[\ ]$ is the Fourier transform
- $G(f_x,f_y,z) = \exp\left[-jkz\sqrt{1-\lambda^2 f_x^2 - \lambda^2 f_y^2}\right]$
- Numerically evaluated using the FFT
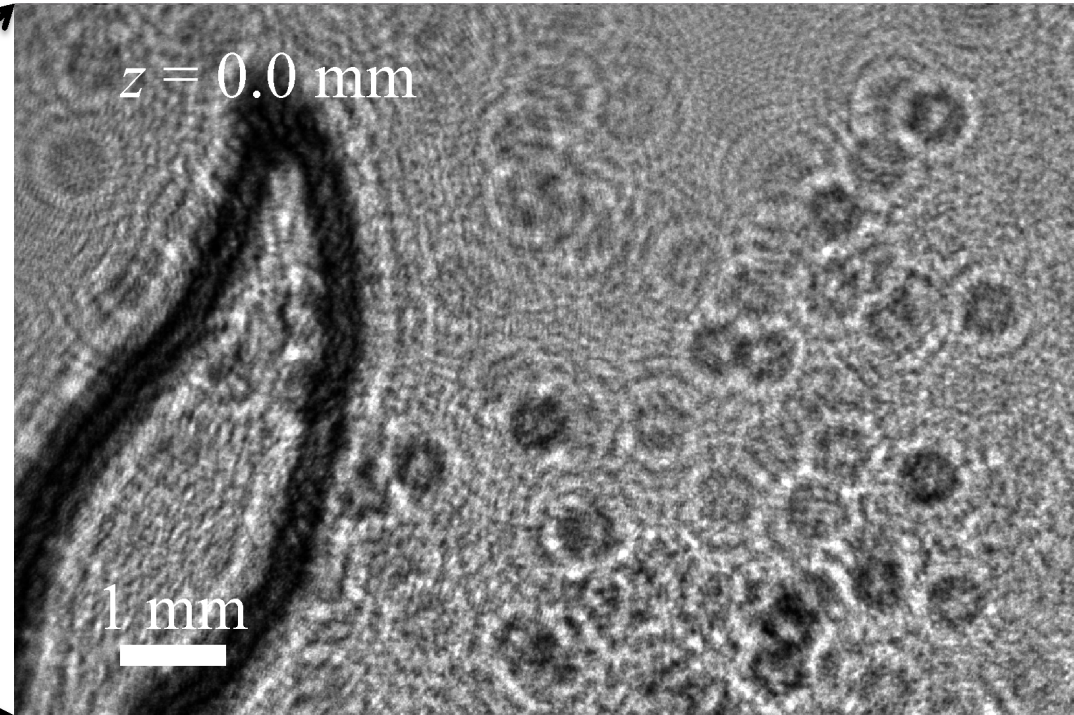- Visualized via the reconstructed amplitude, $A = |E|$, or intensity, $I = |E|^2$

Numerical refocusing

In digital holography, $E(\xi, \eta, 0) = h(\xi, \eta) \cdot E_r^*$

- $h(\xi, \eta)$ = recorded hologram

- E_r^* = complex conjugate of reference wave

  - For a plane reference wave, E_r^* = constant
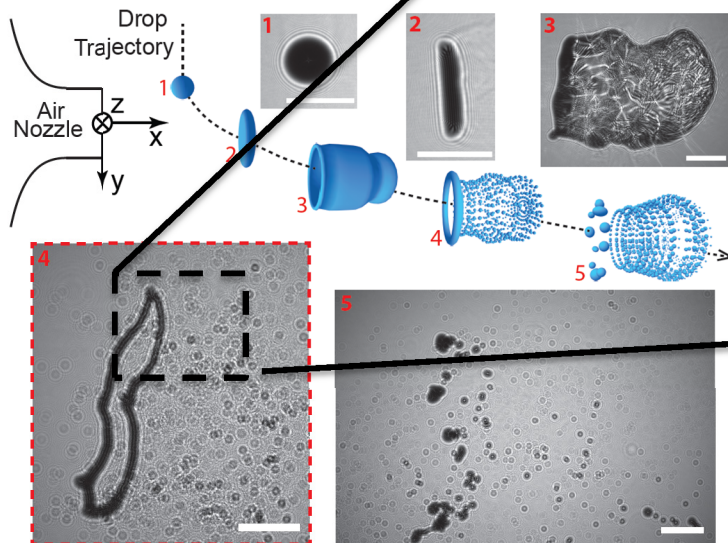
digital holograms of the breakup of an ethanol drop in an air-stream (Gao, Guildenbecher et al 2013, *Opt. Lett.*)

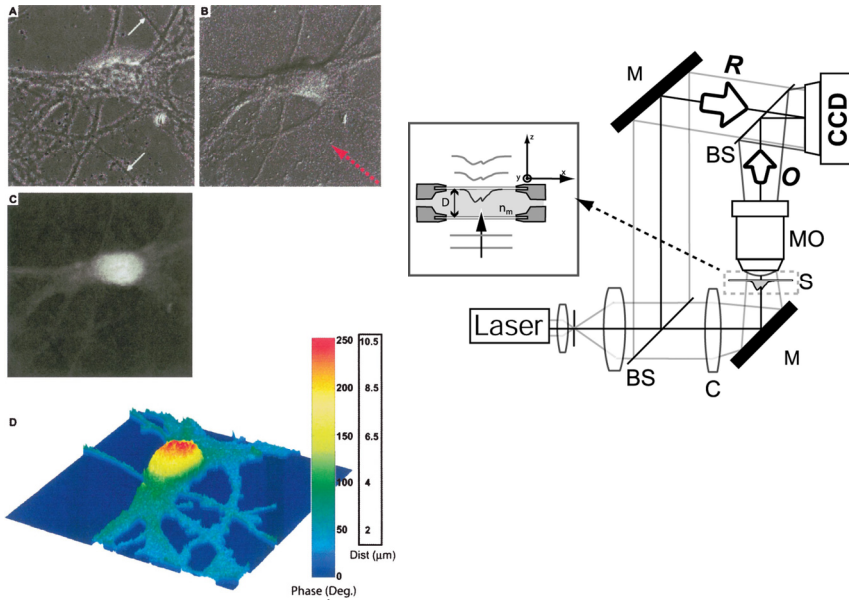$z = 0.0$ mm

1 mm

Reconstructed amplitude throughout depth, z

- In-focus structures are observed at different depths, z

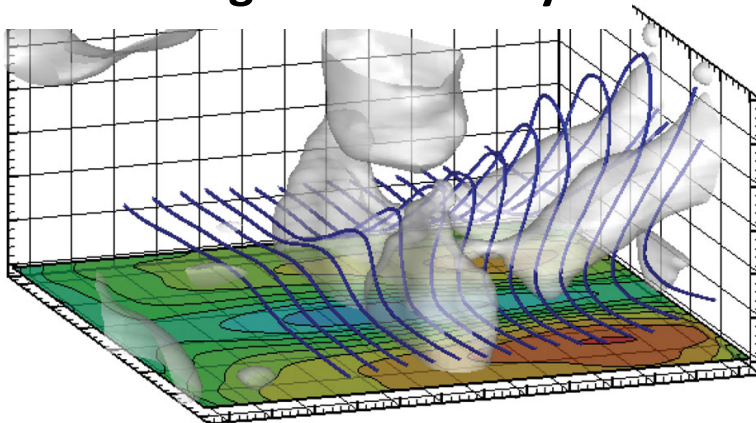- "Rings" around the in-focus structures are the out-of-focus virtual images
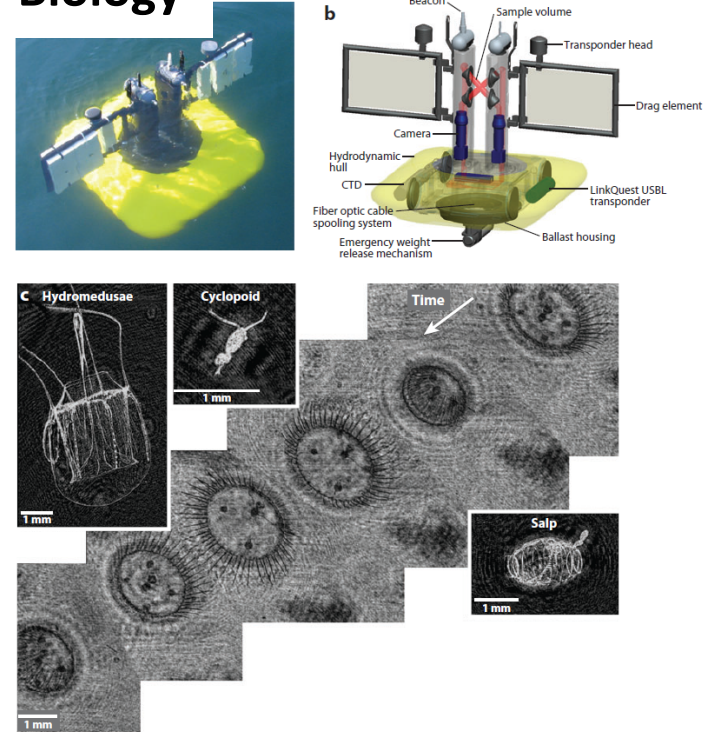
DIH in the literature

Microscopy

Marquet et al 2005, *Opt. Lett.*

Biology

Katz and Sheng 2010, *Annu. Rev. Fluid Mech.*
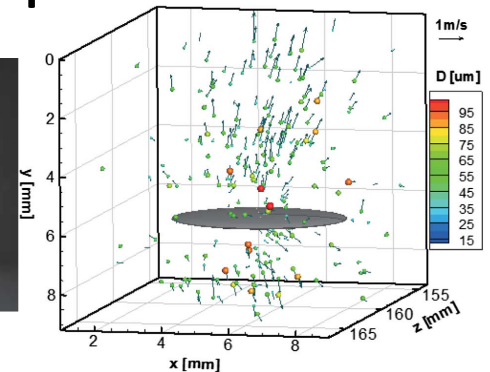
Particle Image Velocimetry

Sheng et al 2009, *J. Fluid Mech.*

Multiphase Flows

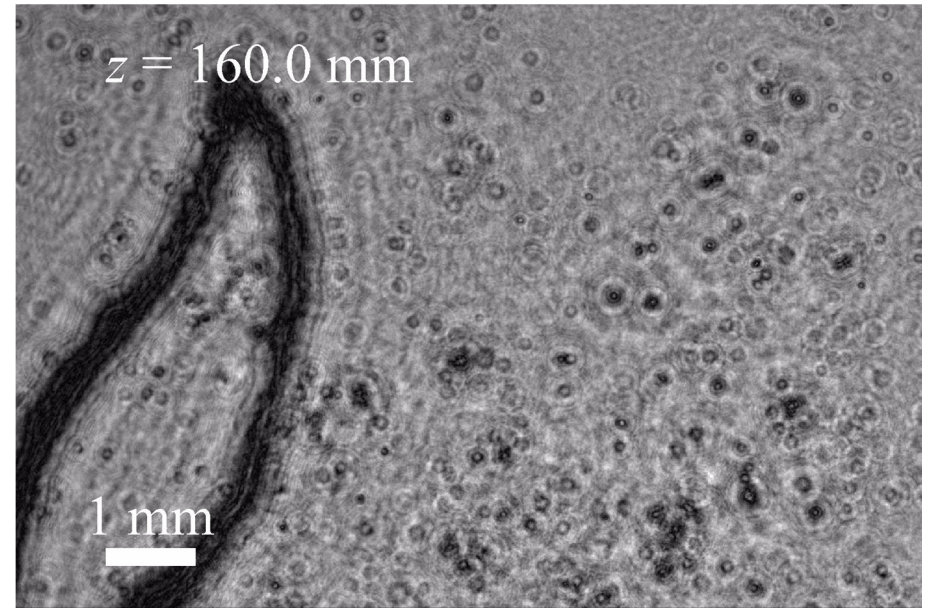Yao et al 2015, *Appl Opt.*

Particle measurements

Data processing

Acquisition and refocusing of a digital hologram is relatively straightforward.

However…

For quantitative measurements, methods are required to locate and measure particles.

$z = 160.0$ mm
1 mm

Challenge: *depth-of-focus problem*

The spatial extent of the diffraction pattern limits the angular aperture, Ω, from which a particle is effectively reconstructed (Meng et al, 2004, *Meas. Sci. Technol.*)

- From the central diffraction lobe → $\Omega \approx 2\lambda/d$

- Using the traditional definition of depth-of-focus, δ, based on change of intensity within the particle center → $\delta \approx 4\lambda/\Omega^2$

- Therefore: for in-line holography, $\delta \approx d^2/\lambda$

    - Example: $d = 300$ μm, $\lambda = 532$ nm → $\delta \approx 170$ mm!

Data processing

Literature contains two basic methods to find the focal plane:

1. Fit a model to the observed diffraction patterns (inverse method)

    ▪ Generally accurate with small depth uncertainty

    ▪ Limited to objects with known diffraction patterns (spheres)

2. Reconstruct the amplitude (or intensity) throughout depth and apply a focus metric to find "in-focus" objects

    ▪ No *a-priori* knowledge of particle shape required

    ▪ Accuracy is a strong function of the chosen focus metric

Hybrid method:

▪ Focus metric is a combination of amplitude minimization and edge sharpness maximization

    ▪ Details in Guildenbecher et al 2013, *Appl. Opt.;* Gao et al 2013, *Opt. Express;* Gao et al 2014, *Appl. Opt.*
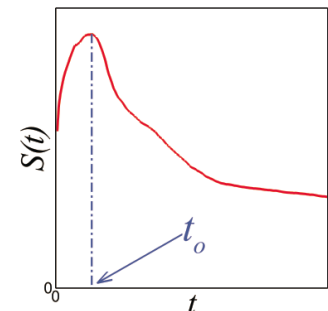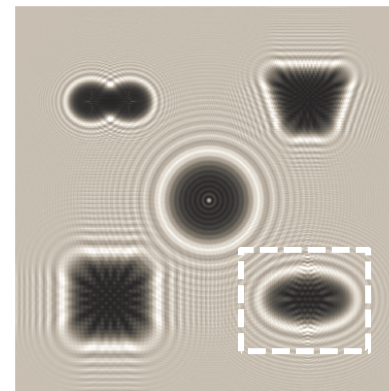
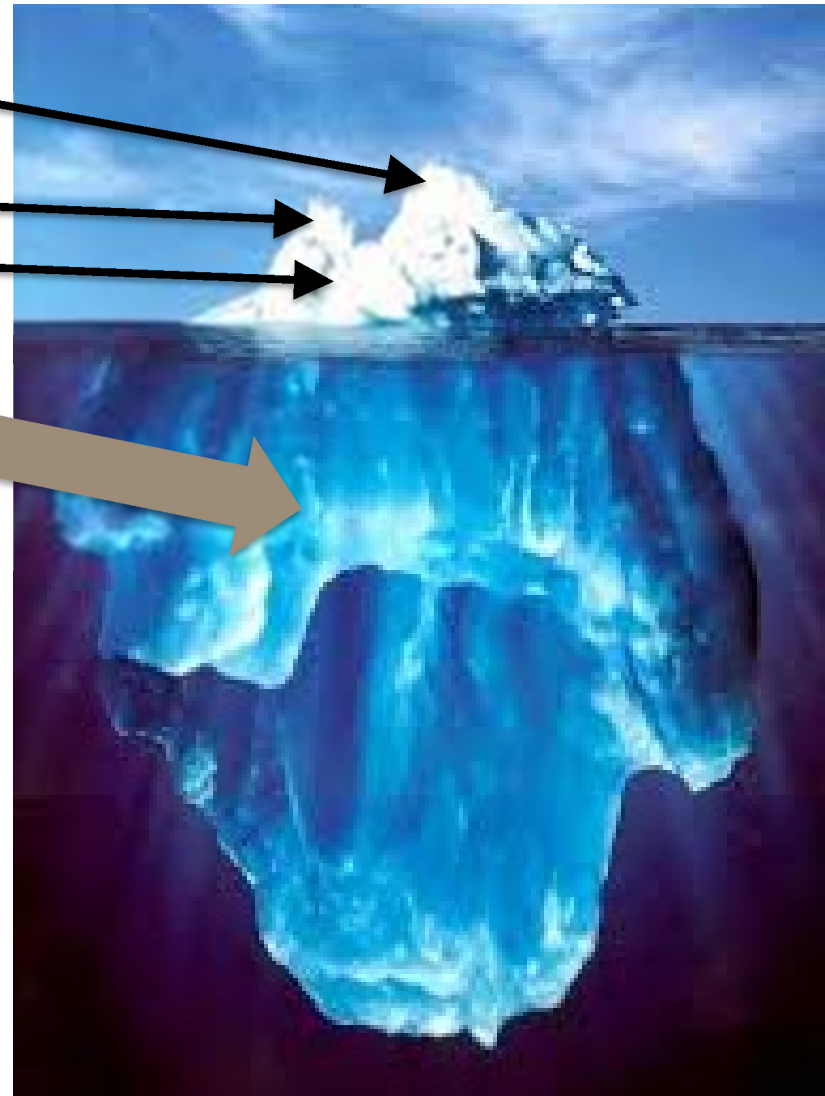Gao et al 2014, *Appl Opt.*

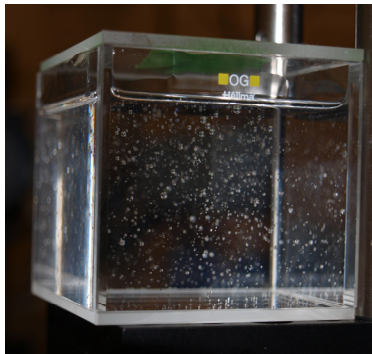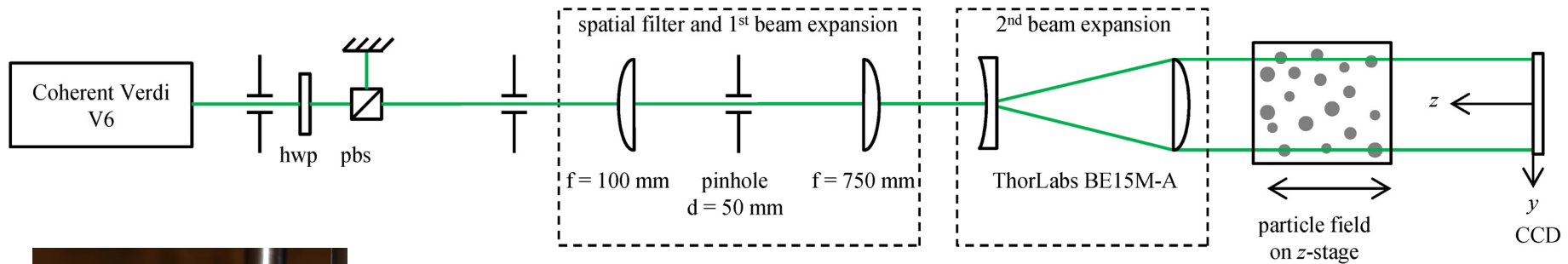# Data processing

The basic DIH system includes:

- Collimated/coherent light source (laser)
- Particle field
- Image recorder (digital camera)

- **DATA ANALYSIS SOFTWARE**

Currently each group has their own code:

- Hybrid : Guildenbecher, Gao, et al
- Laplacian: Choi and Lee
- Correlation coefficient: Yang et al
- Minimum edge intensity: Tian et al
- Variance: Palero et al.
- Etc…

Experimental validation

spatial filter and 1st beam expansion

2nd beam expansion

Coherent Verdi V6

hwp   pbs

f = 100 mm

pinhole
d = 50 mm

f = 750 mm

ThorLabs BE15M-A

particle field
on z-stage

z

y
CCD

particle field

- Quasi-stationary particle field
  - Polystyrene beads ($\bar{d} \approx 465\,\mu m$) in 10,000 cSt silicone oil
  - Settling velocity ≈ 0.8 μm/s
- Multiple holograms recorded, displacing the particle field 2 mm in the z-direction between each acquisition

2 mm
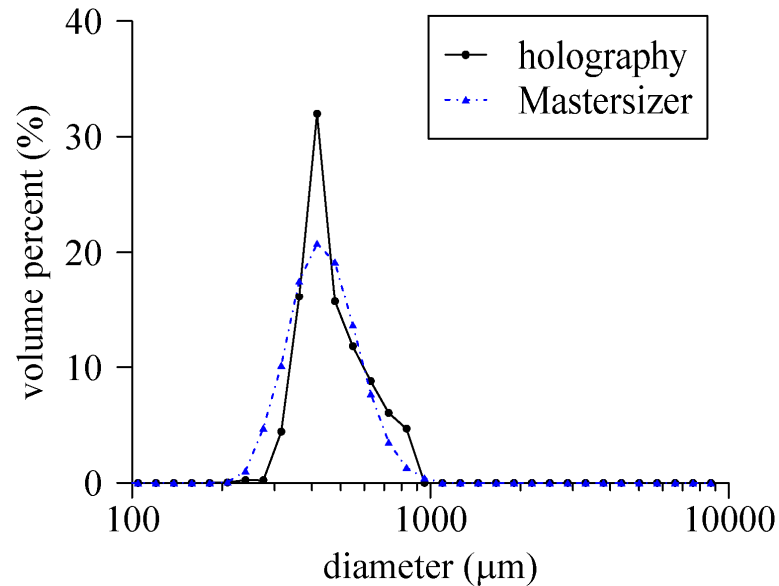
hologram
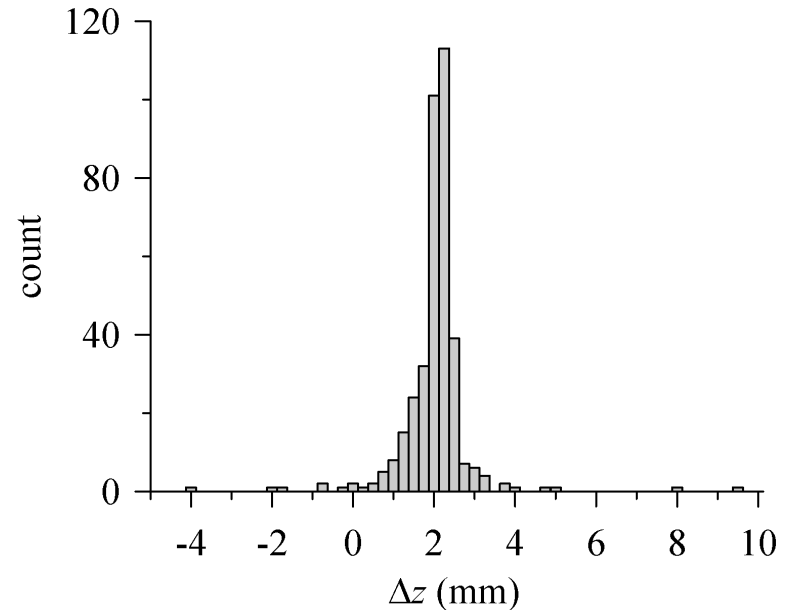
2 mm

object z [mm]

210
205
200
195
190
185
180
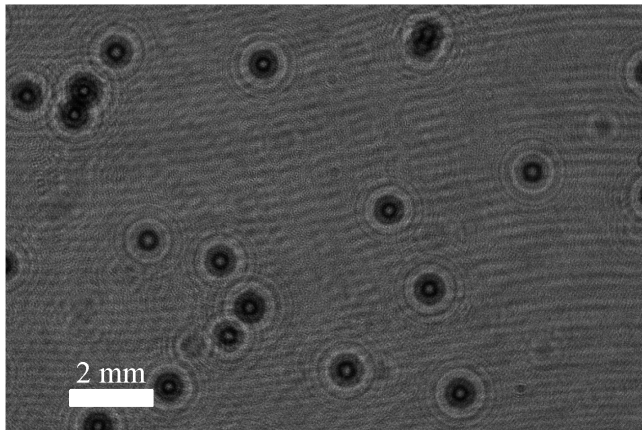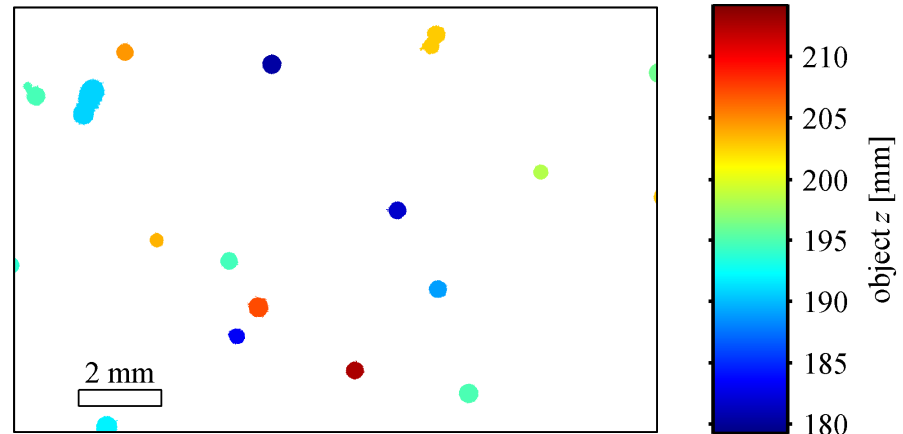
Detected objects colored by z-position

Experimental validation

Diameter measured from area of the detected 2D morphology

- Actual mass median diameter = 465 μm

- Measured mass median diameter = 474 μm

 - Error of 2.0% with respect to actual value

Displacement found by particle matching between successive holograms

- Actual displacement = 2.0 mm

- Mean detected displacement = 1.91 mm +/- 0.81 mm

  - Standard deviation of 1.74 times mean diameter

Aerodynamic drop fragmentation

Experimental configuration: Double-pulsed laser and imaging hardware as typically used in PIV

- λ = 532 nm, 5 ns pulsewidth

- Interline transfer CCD (4008 × 2672, 9 μm pixel pitch)
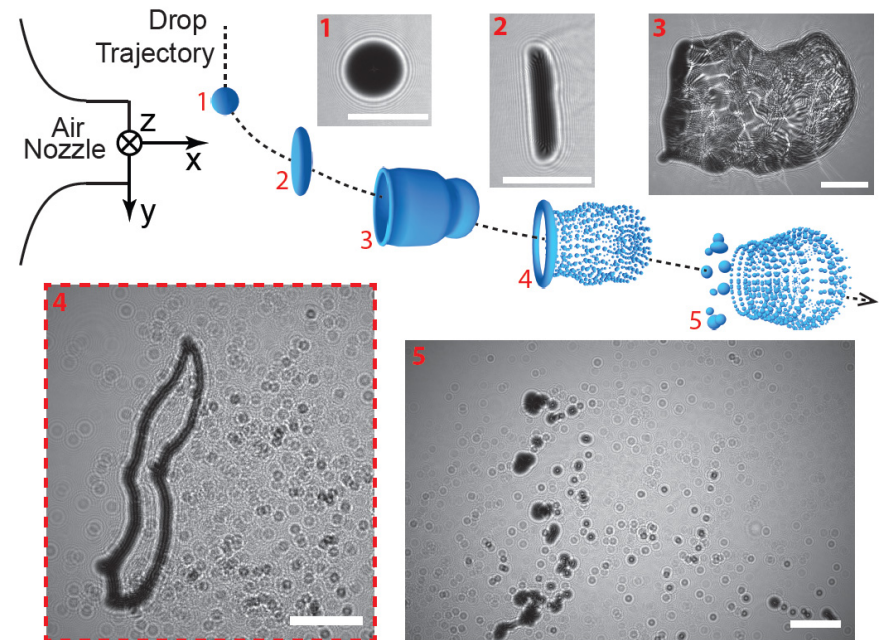
- Temporal separation, Δt = 62 μs, determined by laser timing

digital holograms of the breakup of an ethanol drop in an air-stream (Gao, Guildenbecher et al 2013, *Opt. Lett.*)

Note: without a separate reference wave, coherence length requirements in DIH are greatly relaxed.

- Expensive injection seeders are not always needed

- Faster lasers (ps or fs) can be used with some advantages (e.g. Nicolas et al 2007, *Opt. Express*)

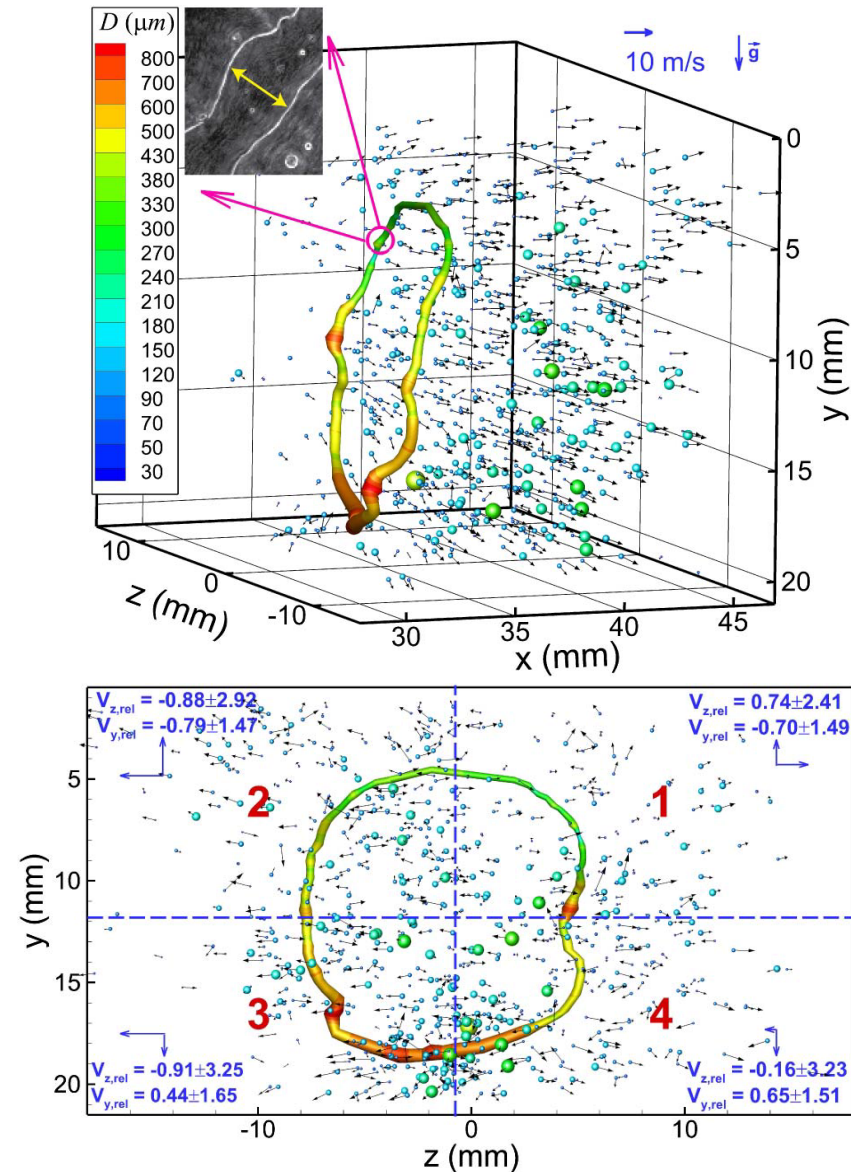# Aerodynamic drop fragmentation

Secondary drop sizes/positions extracted by the hybrid method

- Comparison with phase Doppler anemometer (PDA) data confirms accuracy of measured sizes
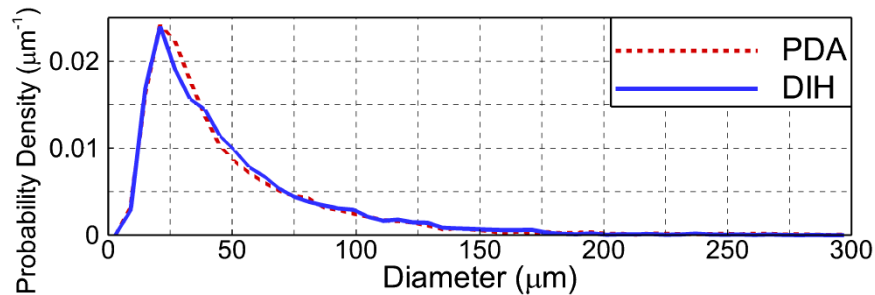
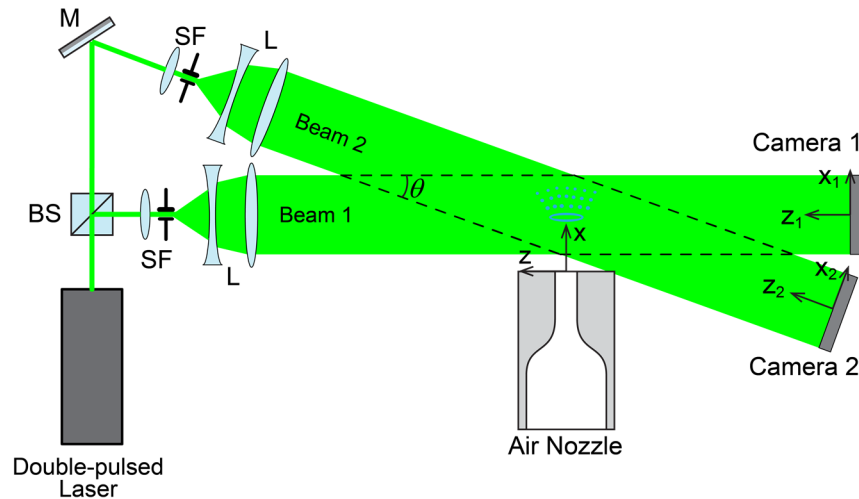Ring measured from z-location of maximum image gradient

- Total volume of ring + secondary drops is within 2.2% of the initial volume

Aerodynamic drop fragmentation

Velocimetry suffers from uncertainty in the out-of-plane (z) position
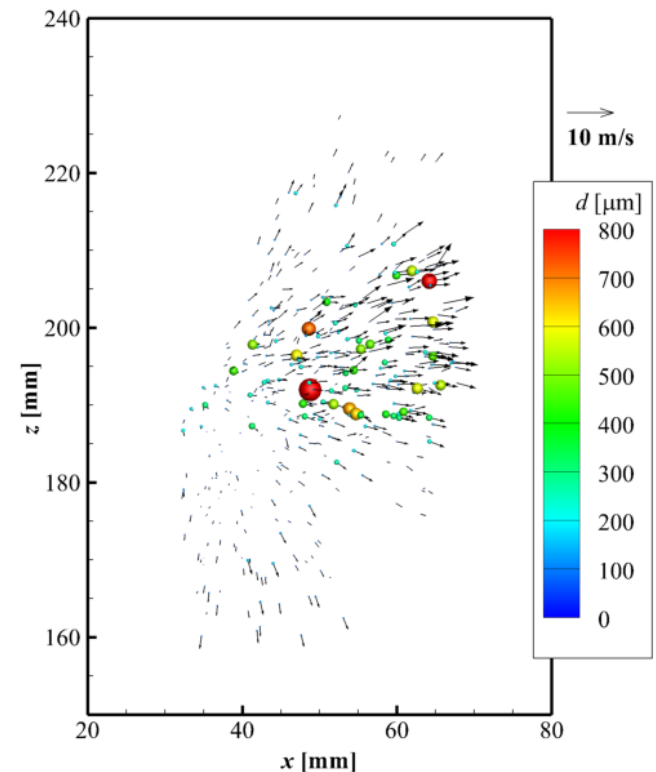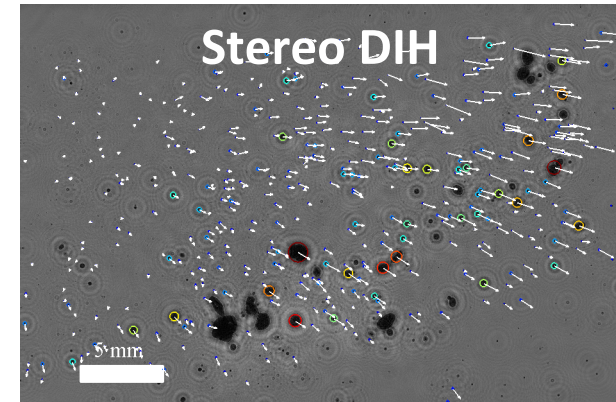
- A stereo-view configuration is one solution

Stereo DIH

Advantages:
- Improved z-uncertainty
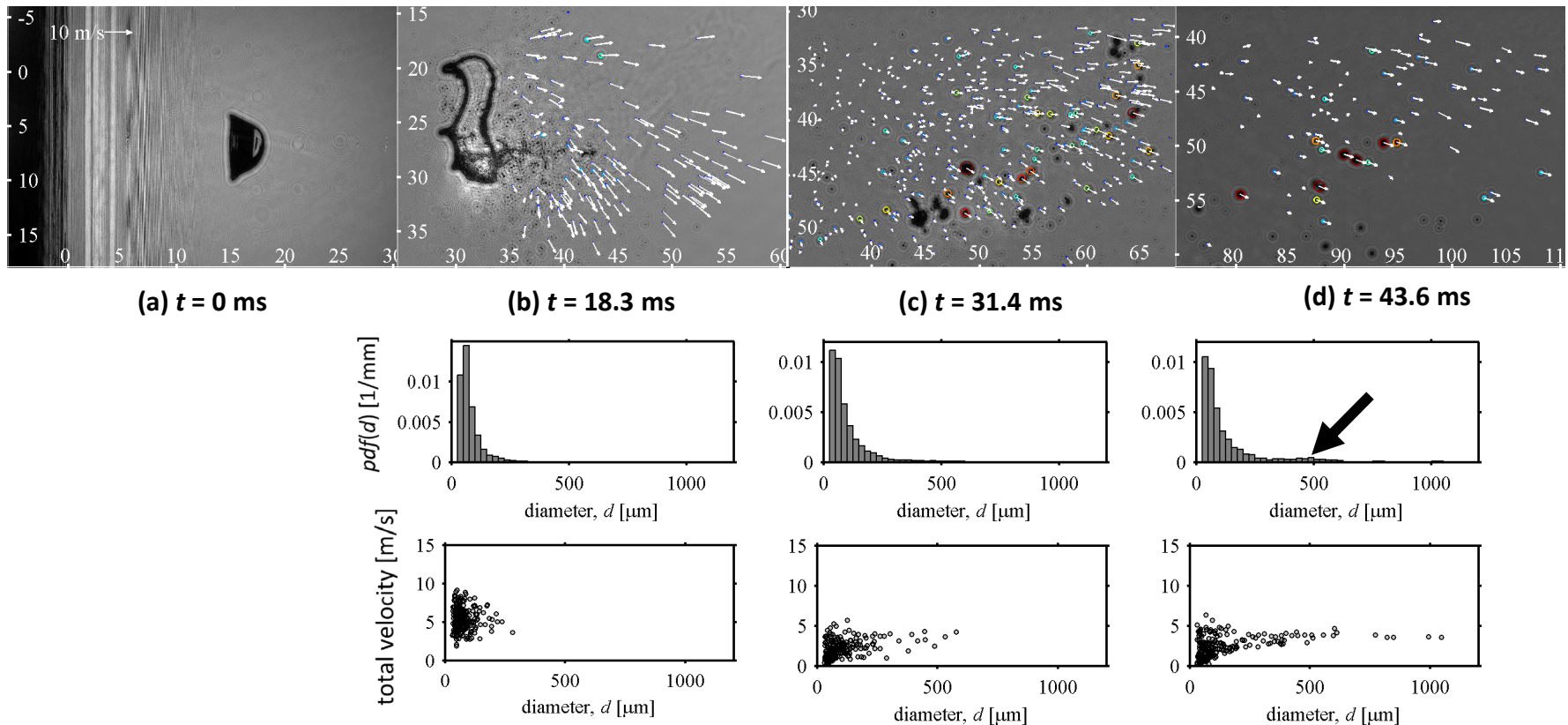- Eliminates false particle size and position measurements

Challenges:
- Increased experimental complexity
- Careful calibration required

Aerodynamic drop fragmentation
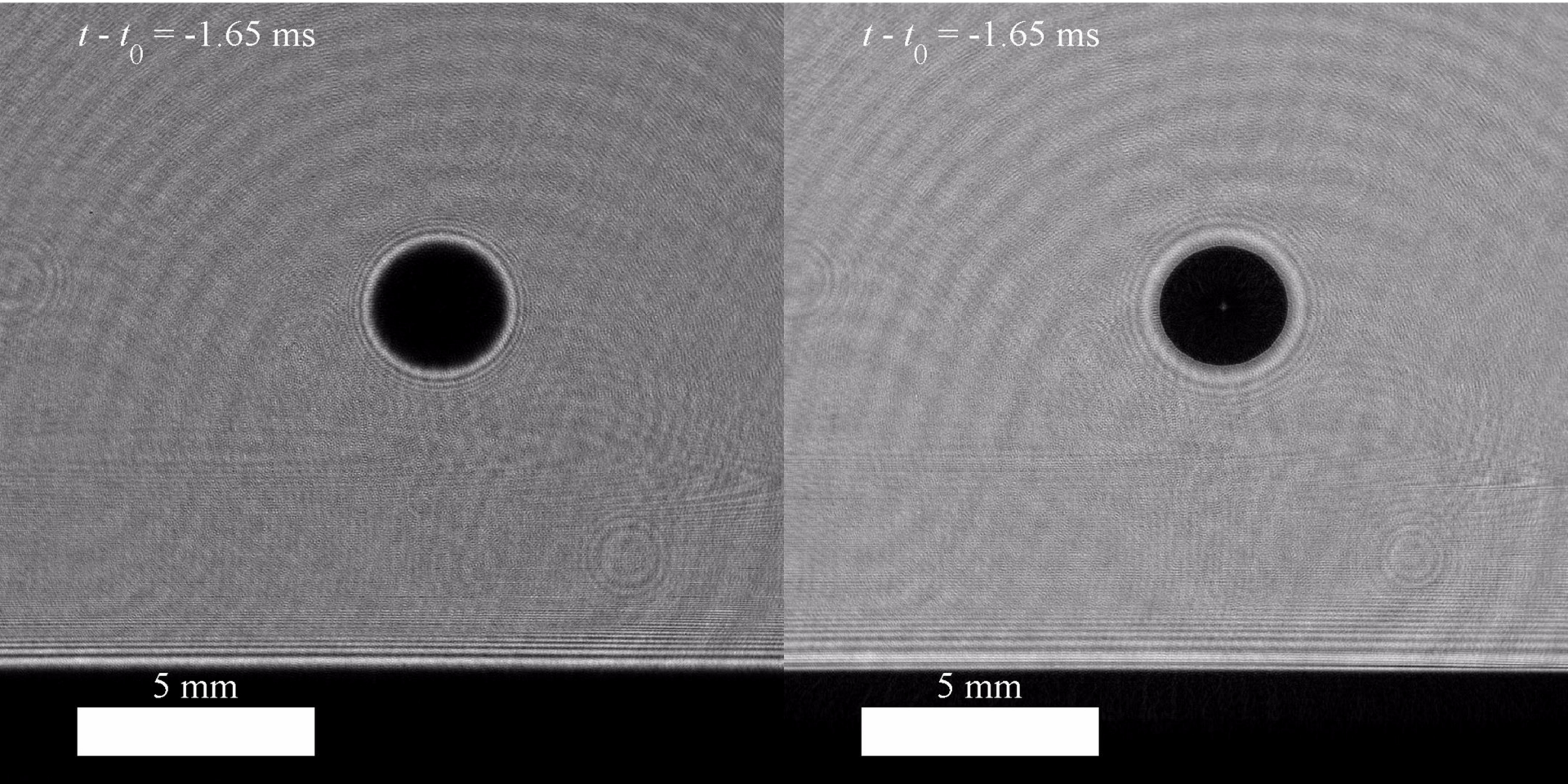
Ensemble averaging of 44 realizations at each condition

- Roughly 10,000 individual drops measured per condition

(a) *t* = 0 ms   (b) *t* = 18.3 ms   (c) *t* = 31.4 ms   (d) *t* = 43.6 ms

DIH is particularly advantageous for rapid quantification of particle statistics

High-speed (kHz) DIH

Increased temporal resolution is possible using high-speed (kHz rate) cameras

$t - t_0 = -1.65$ ms

$t - t_0 = -1.65$ ms

5 mm

5 mm

<u>Challenges:</u> (1) higher readout noise, fewer pixels, larger pixel pitches
(2) very large data sets (10s of Gb)

High-speed (kHz) DIH

Processing of a single hologram can take roughly 30 min on a typical CPU

- Much of that time spent on numerical refocusing:

$$E(x,y,z) = FFT^{-1}\Big[FFT\big[h(\xi,\eta) \big] \cdot G\big(f_x, f_y, z \big) \Big]$$

  - Refocusing to a single depth requires:

    (1) calculation of $G(f_x, f_y, z)$

    (2) multiplication of two large arrays, $FFT[h(\xi,\eta)] \cdot G(f_x, f_y, z)$

    (3) a two-dimensional inverse FFT

Graphical processing units (GPUs) are well suited to these tasks

- E.g. NVIDIA Tesla K40 GPU, Dual Xeon CPU, Matlab v2014a with parallel computing toolbox → *per-frame processing time of ~7 seconds*
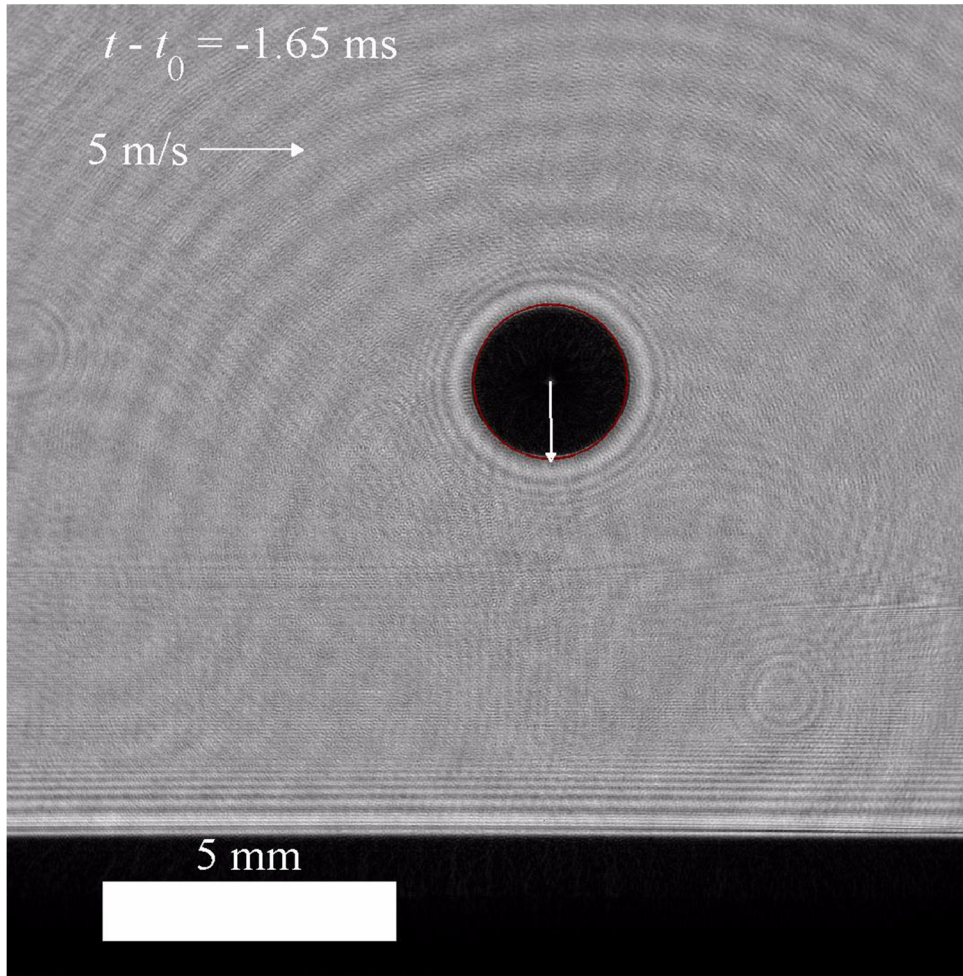
High-speed (kHz) DIH
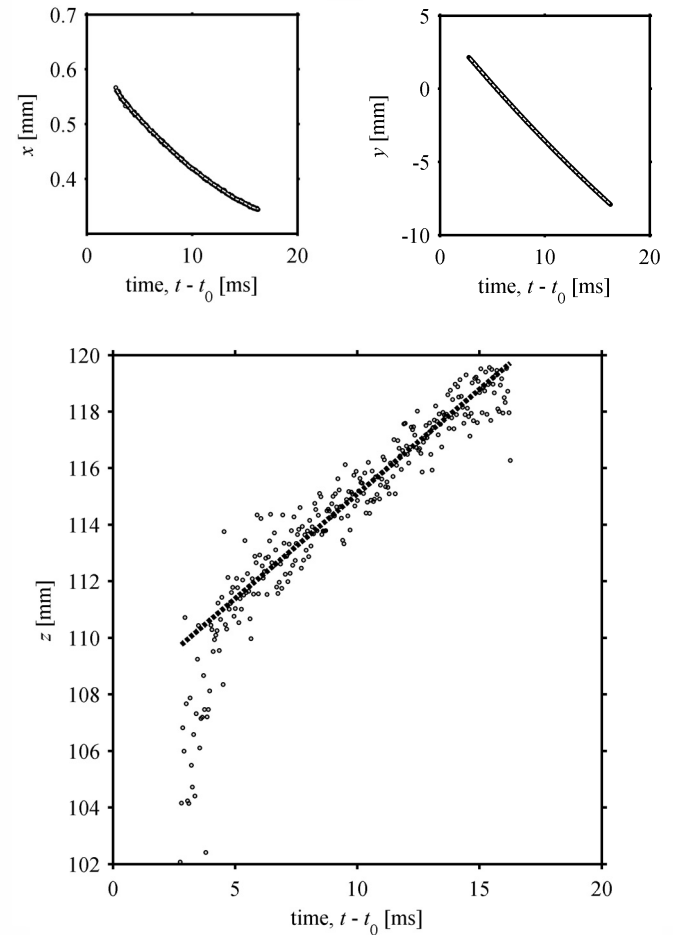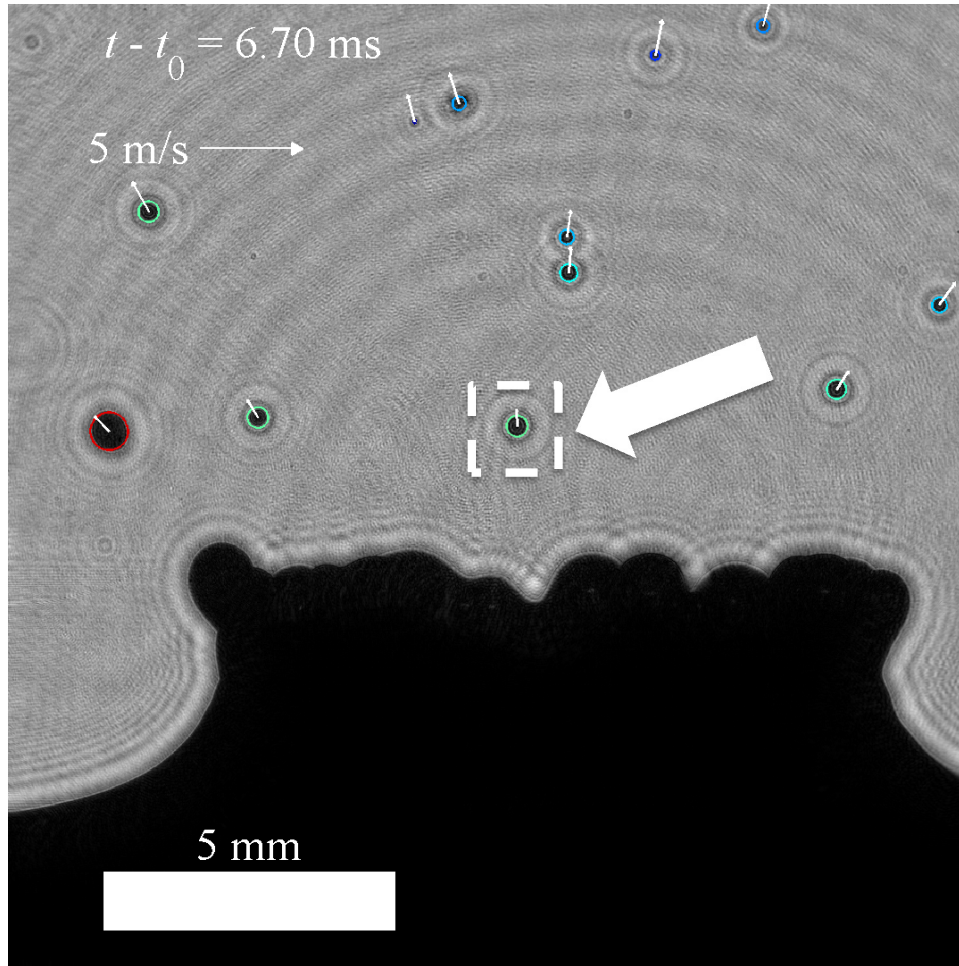
- Frame-to-frame particle matching illustrates the depth-of-focus problem
- With sufficient temporal resolution, particles trajectories can be fit to temporal models
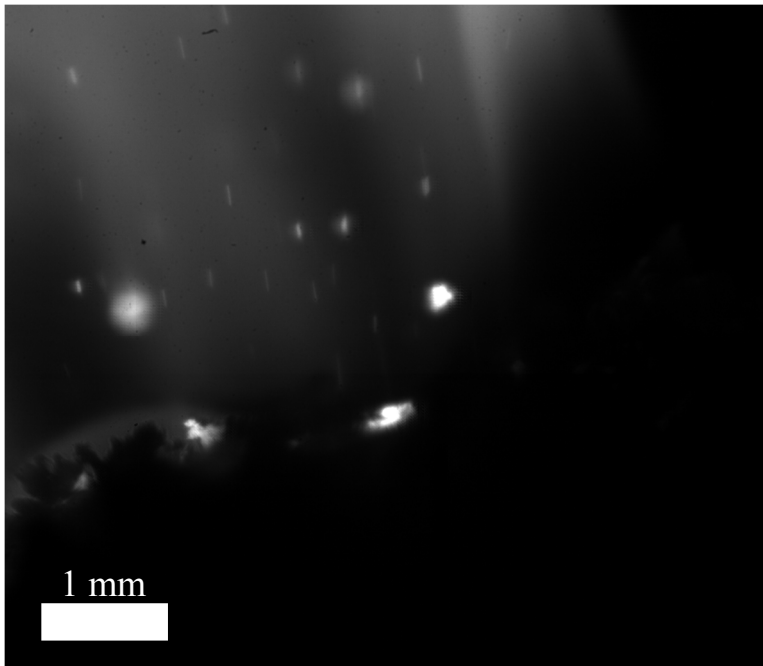
High-speed (kHz) DIH

$t - t_0 = -1.65$ ms

5 m/s →

5 mm
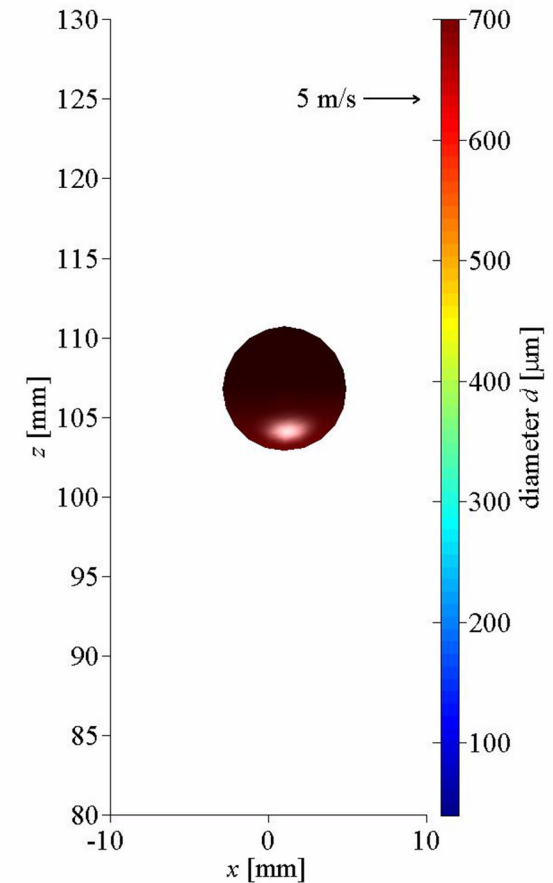
- Multi-frame trajectory fitting leads to a 36X reduction in z-uncertainty

Aluminum drop combustion in propellants

Motivation: rocket failures can lead to propellant fires

- Sandia Laboratories is interested in predicting the response of objects in this environment

http://www.cbsnews.com/news/rocket-crash-no-immediate-threat-to-station-but-cause-is-unknown/

1 mm

high-speed video of a burning propellant

Aluminum agglomeration at the surface yields large reacting drops with high damage potential

- Prediction requires knowledge of particle *size*, *velocity*, and *temperature*

Aluminum drop combustion in propellants
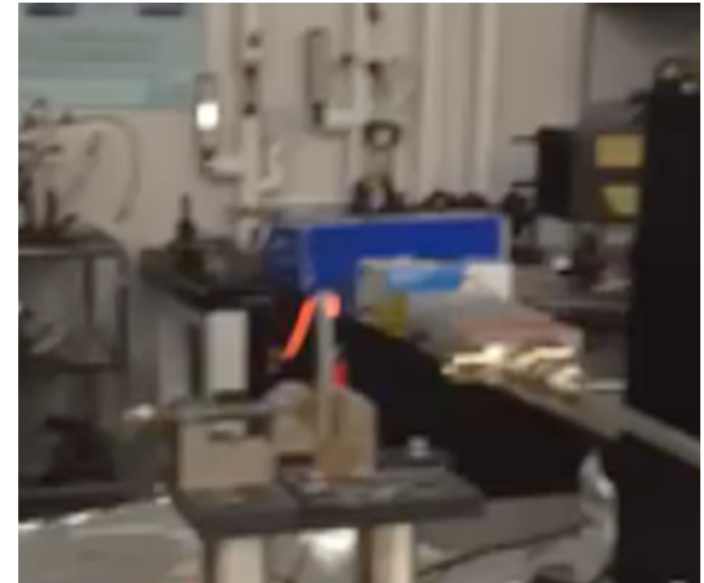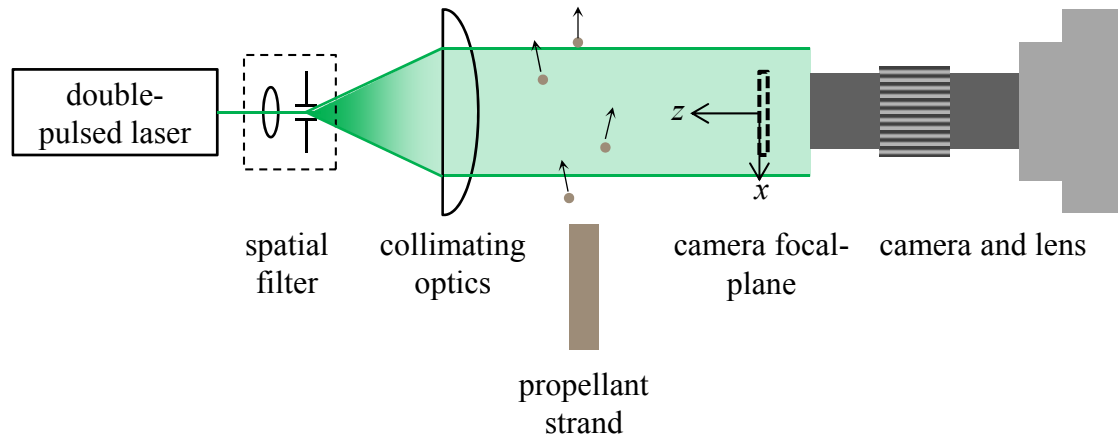
propellant in the text fixture

Propellant: solid-rocket propellant pressed into a pencil size strand

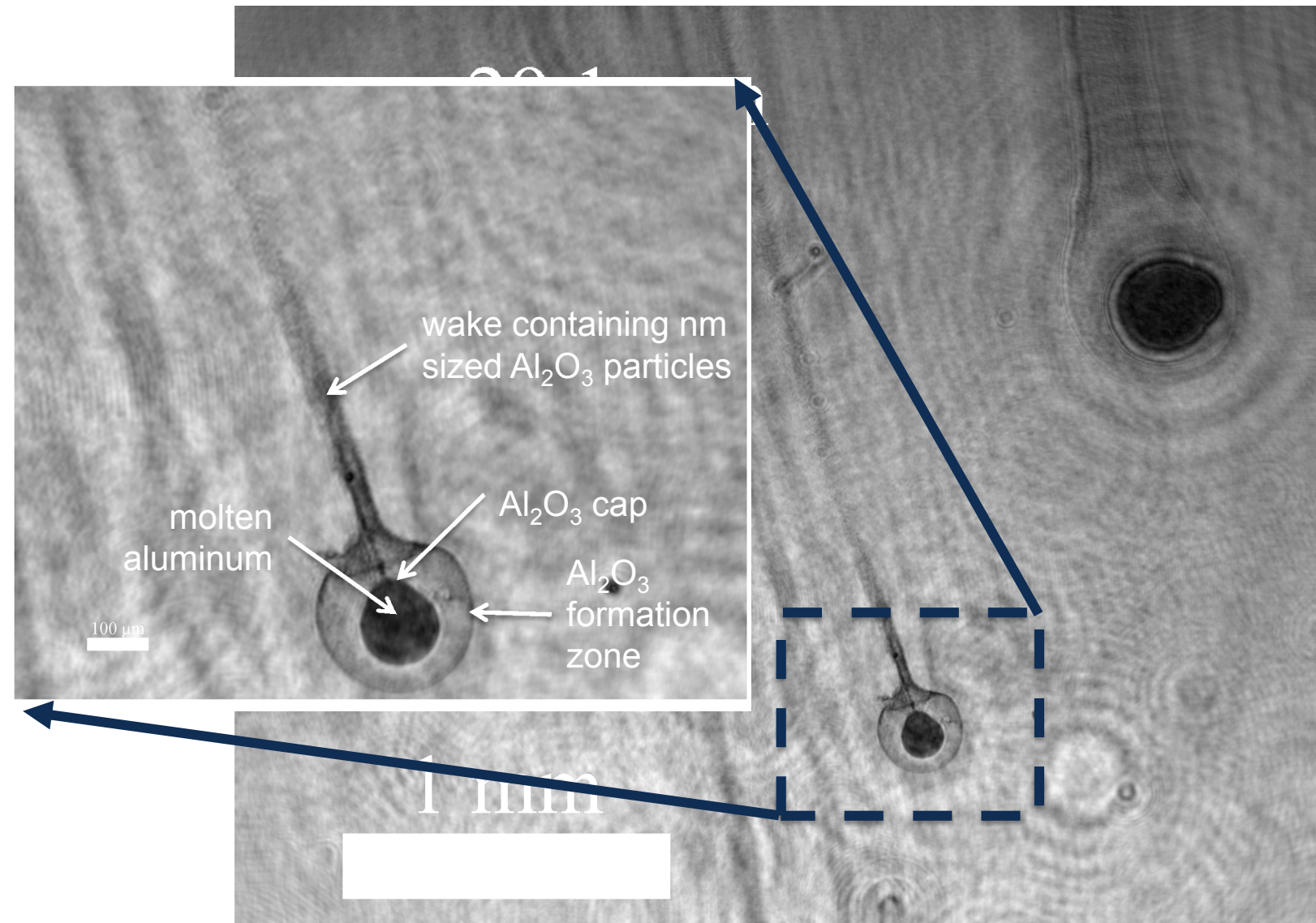- Combusts from the top surface down, ejecting molten aluminum particles traveling a few m/s

Laser: Continuum Minilite Nd:YAG, 532 nm wavelength, 5 ns pulse duration
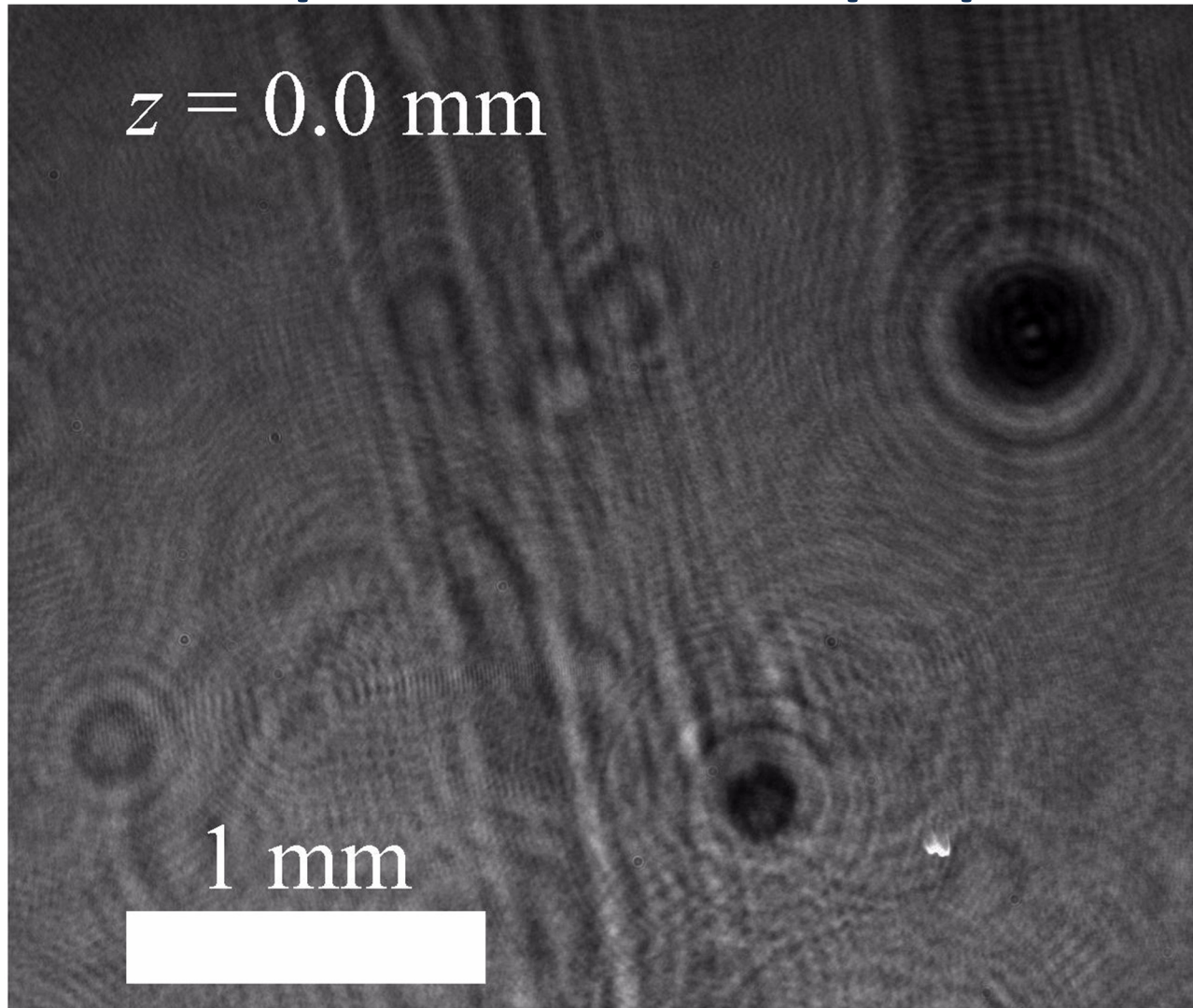
Camera: sCMOS from LaVision at 15Hz

Lens: Infinity K2 long distance microscope with CF-4 objective

- ~ 6X magnification

Aluminum drop combustion in propellants

wake containing nm sized Al_2O_3 particles

molten aluminum

Al_2O_3 cap

Al_2O_3 formation zone

100 µm

1 mm

Aluminum drop combustion in propellants

$z = 0.0$ mm

1 mm

Algorithms automatically measure unique features of burning aluminum

Aluminum drop combustion in propellants

Three strand burns → 5594 images and 17496 measured drops

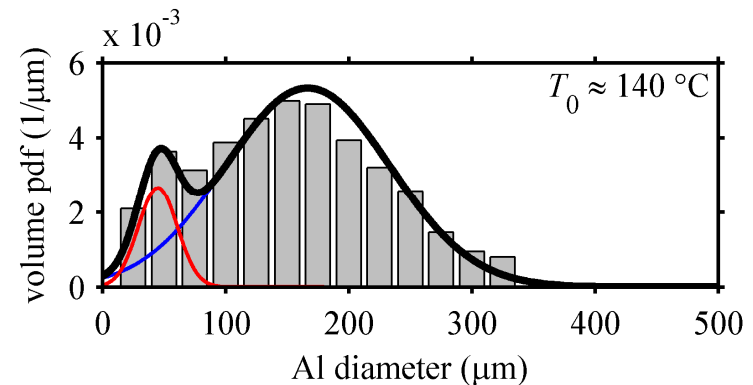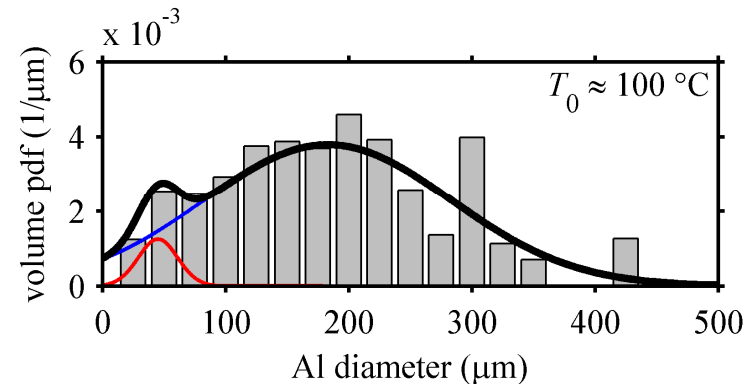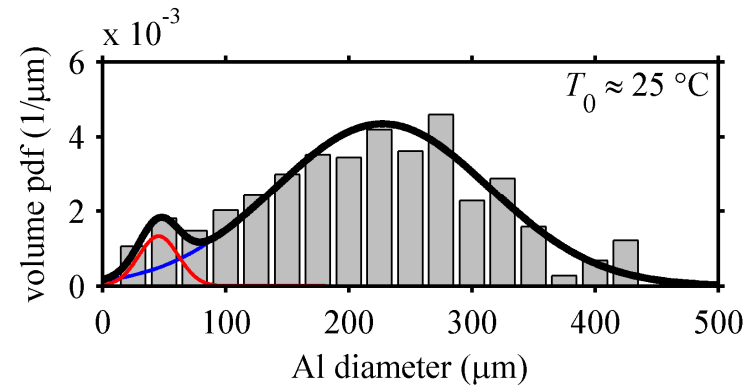- Main peak due to agglomerated particulates
- Peak at 50 μm due to non-agglomerated particulate

Experiments repeated at higher initial temperature (faster burn rate)

- Main peak is reduced due to decreased residence time for agglomeration
- Peak at 50 μm remains

Trend is consistent at still higher initial temperatures
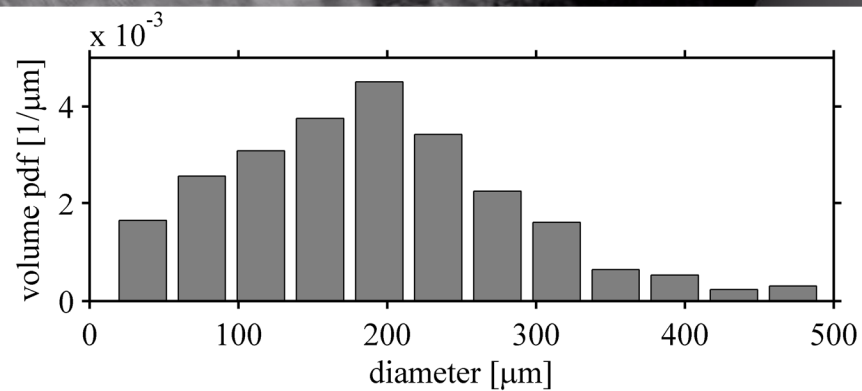
- Main peak reduced further
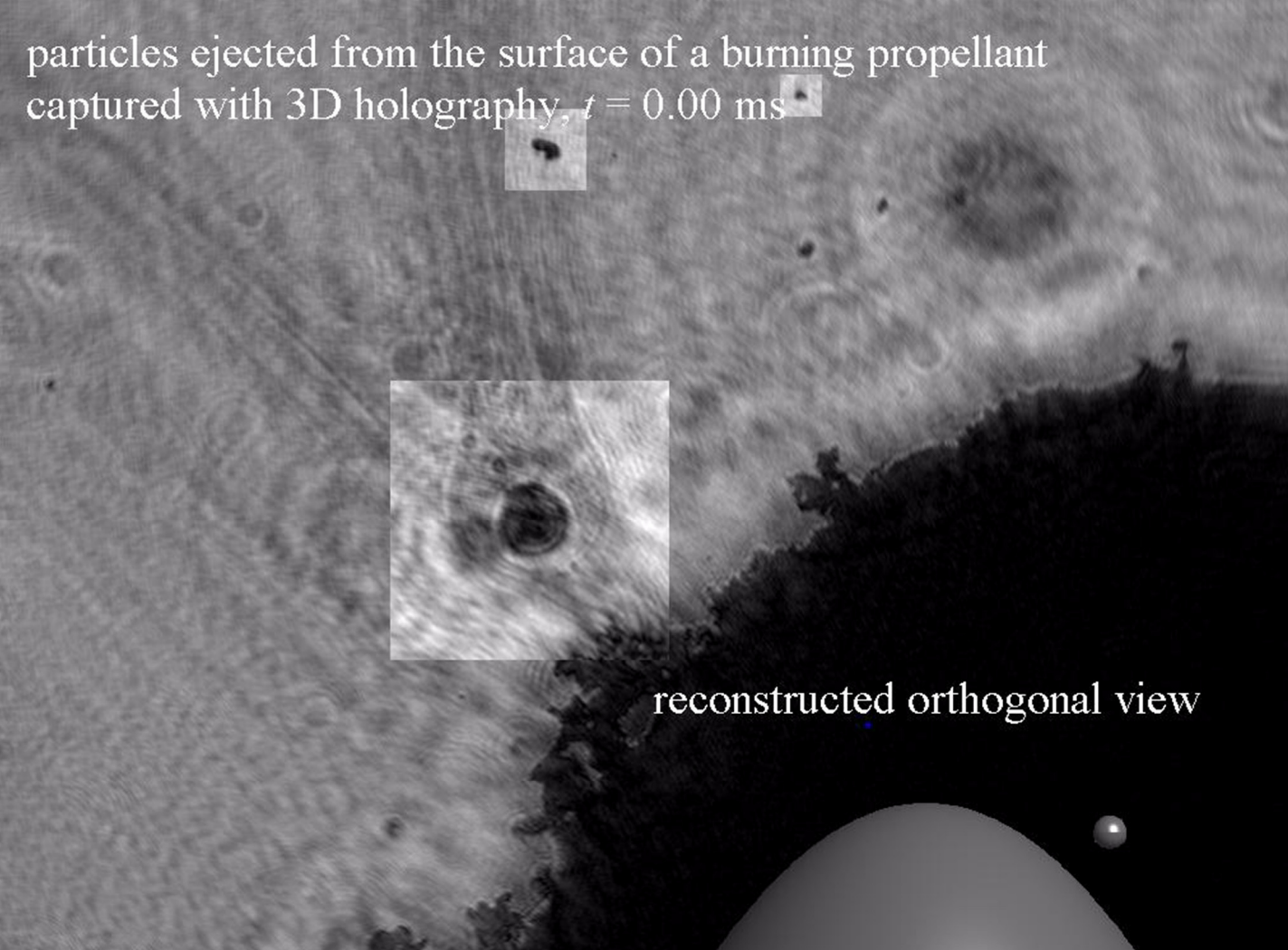- Peak at 50 μm remains

particles ejected from the surface of a burning propellant captured with 3D holography, $t = 0.00$ ms

reconstructed orthogonal view

Sandia National Laboratories

Recorded at 20,000 fps

Camera: Photron SA-Z

Laser: Coherent Verdi V6
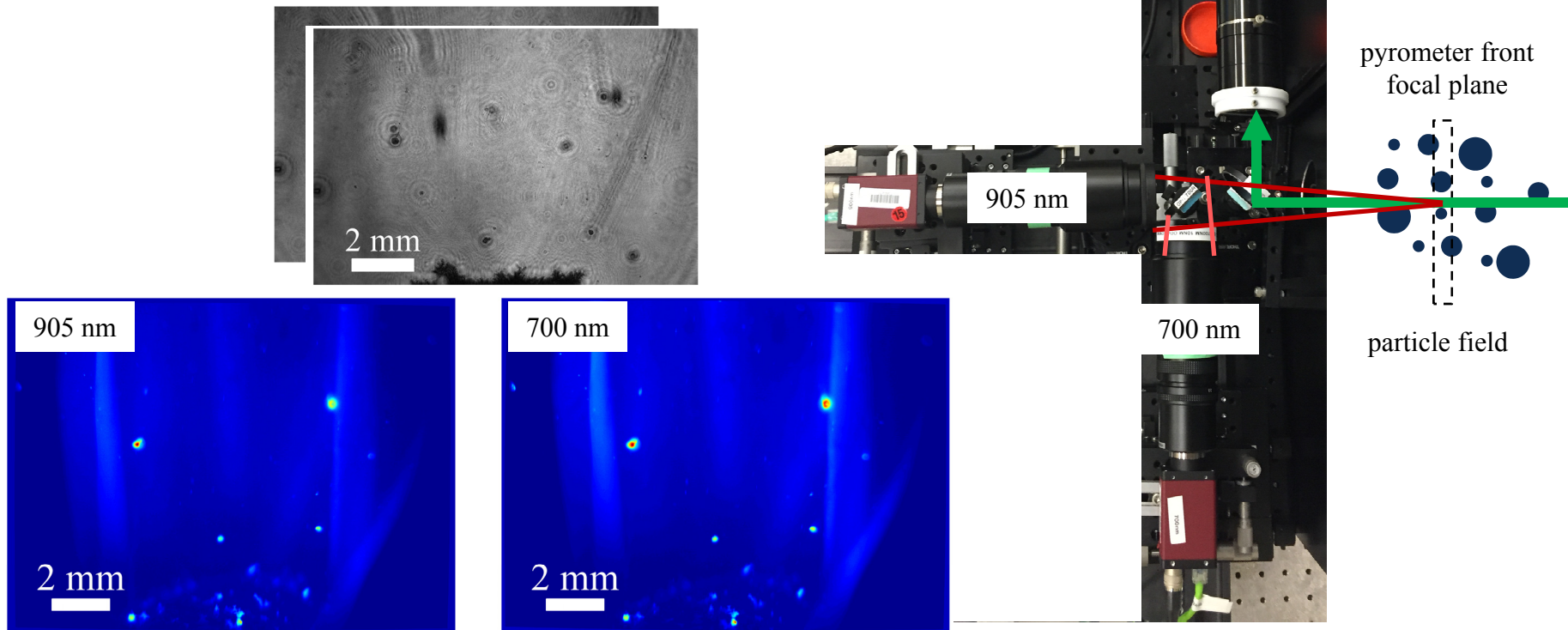
43,684 frames → 15,991 measured drops
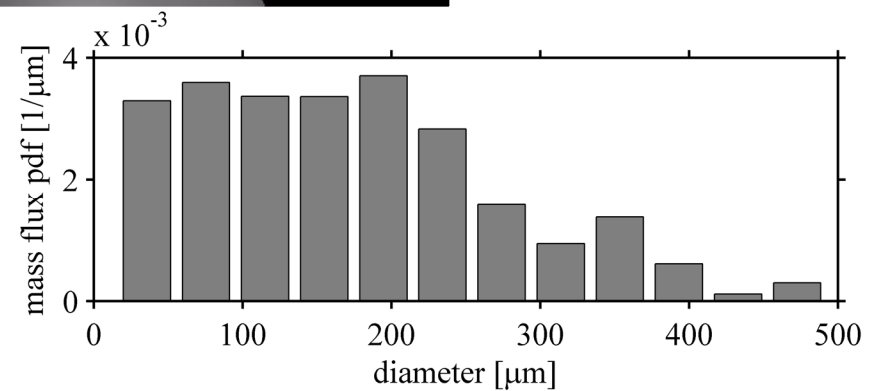
Aluminum drop combustion in propellants

DIH gives mass transfer (particle size + velocity)

We really need to quantify the heat transfer (particle and gas phase)

- Combination of DIH and two-color pyrometery → particle size + velocity + *temperature*

2 mm

905 nm

2 mm

700 nm

2 mm

905 nm

700 nm

pyrometer front focal plane

particle field

Aluminum drop combustion in propellants

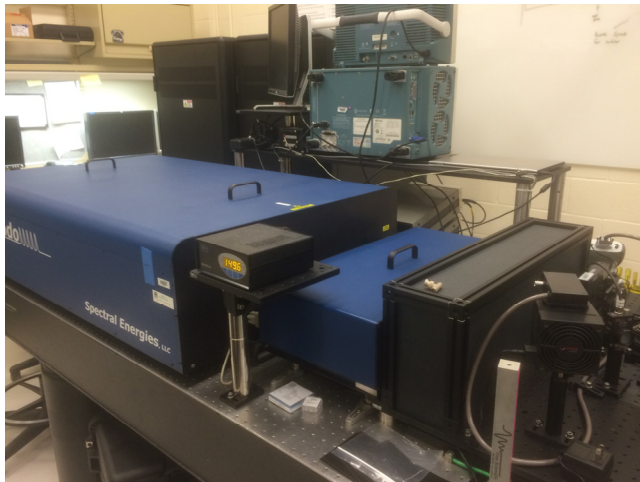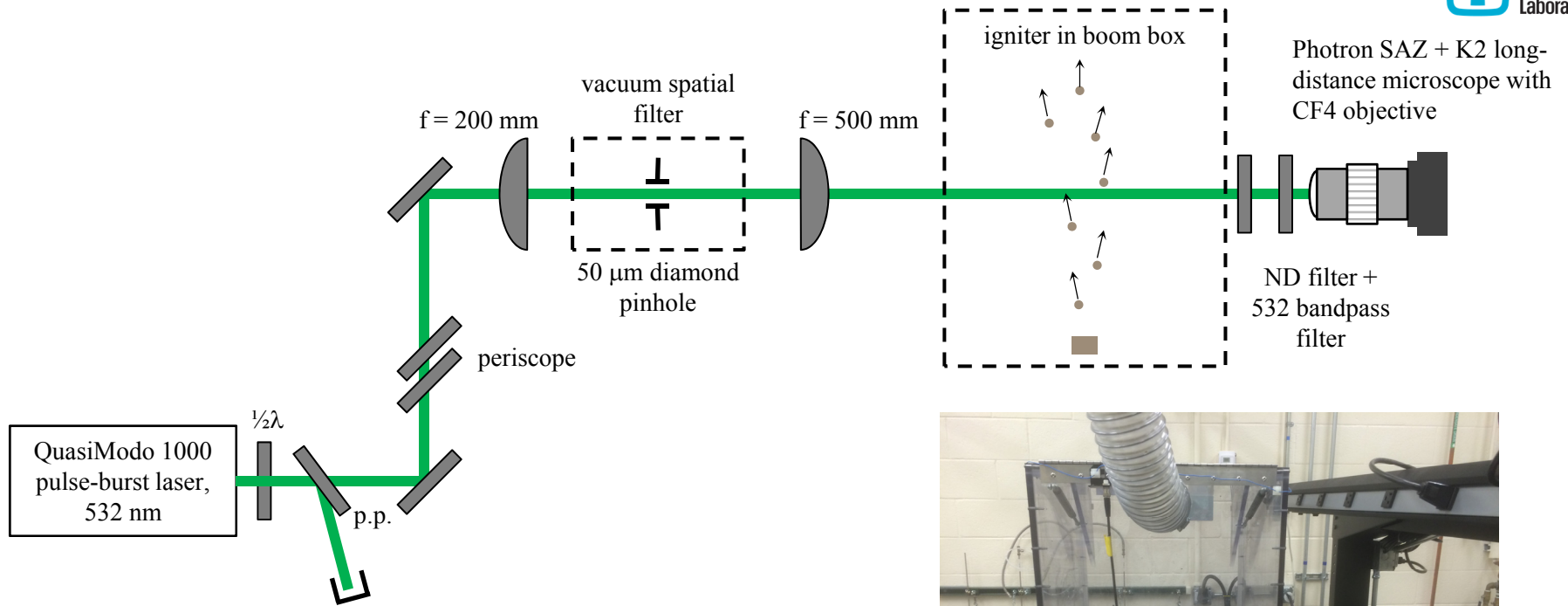Gas phase temperature can be measured using fs/ps CARS

- Advantages compared to ns CARS:

  - Low (mJ) pulse energies → reduces dielectric breakdown

  - Time-delayed probe → eliminates background signal

  - Enhanced precision ~ 1%
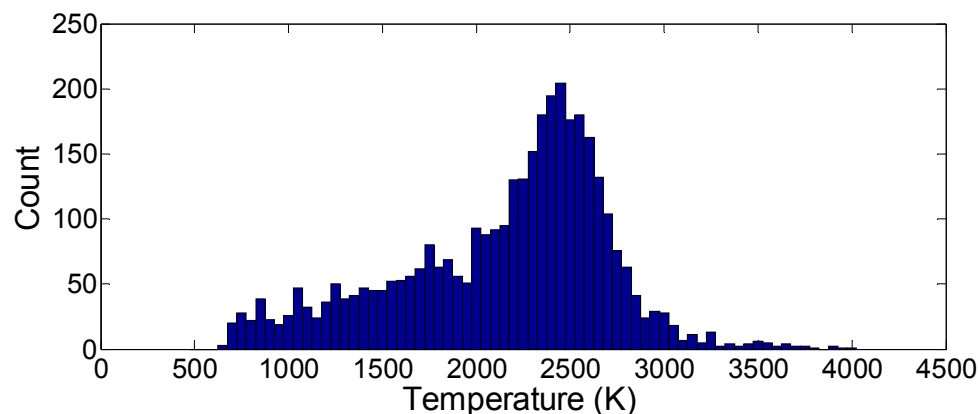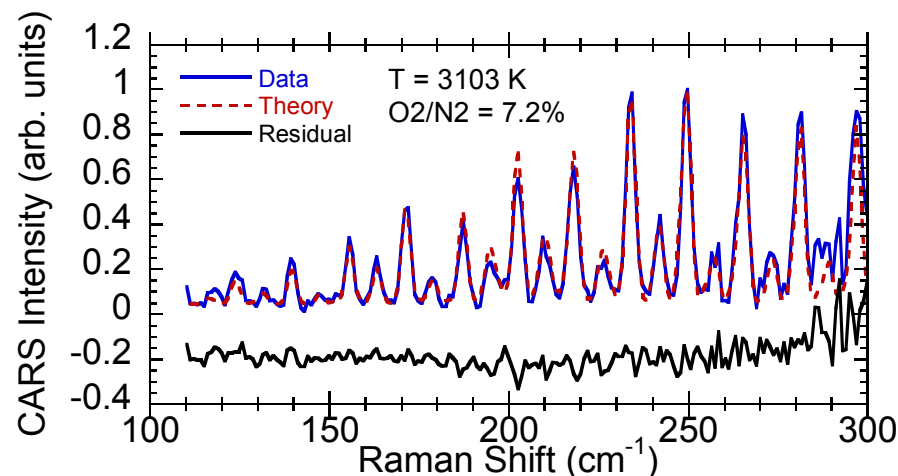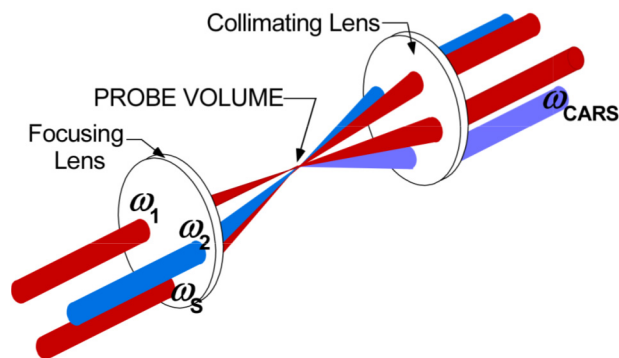
See poster: *Hybrid fs/ps CARS for sooting and metalized flames* by Kathryn Hoffmeister, Sean Kearney, Daniel Guildenbecher, and Caroline Winters

# New concepts and opportunities

Pulse-burst DIH

f = 200 mm

vacuum spatial filter

50 μm diamond pinhole

f = 500 mm

igniter in boom box

Photron SAZ + K2 long-distance microscope with CF4 objective

ND filter + 532 bandpass filter

periscope

½λ

QuasiModo 1000 pulse-burst laser, 532 nm

p.p.

Spectral Energies pulse-burst laser

boom-box and high-speed DIH imager

Pulse-burst DIH

$t = 0.00$ ms

1 mm
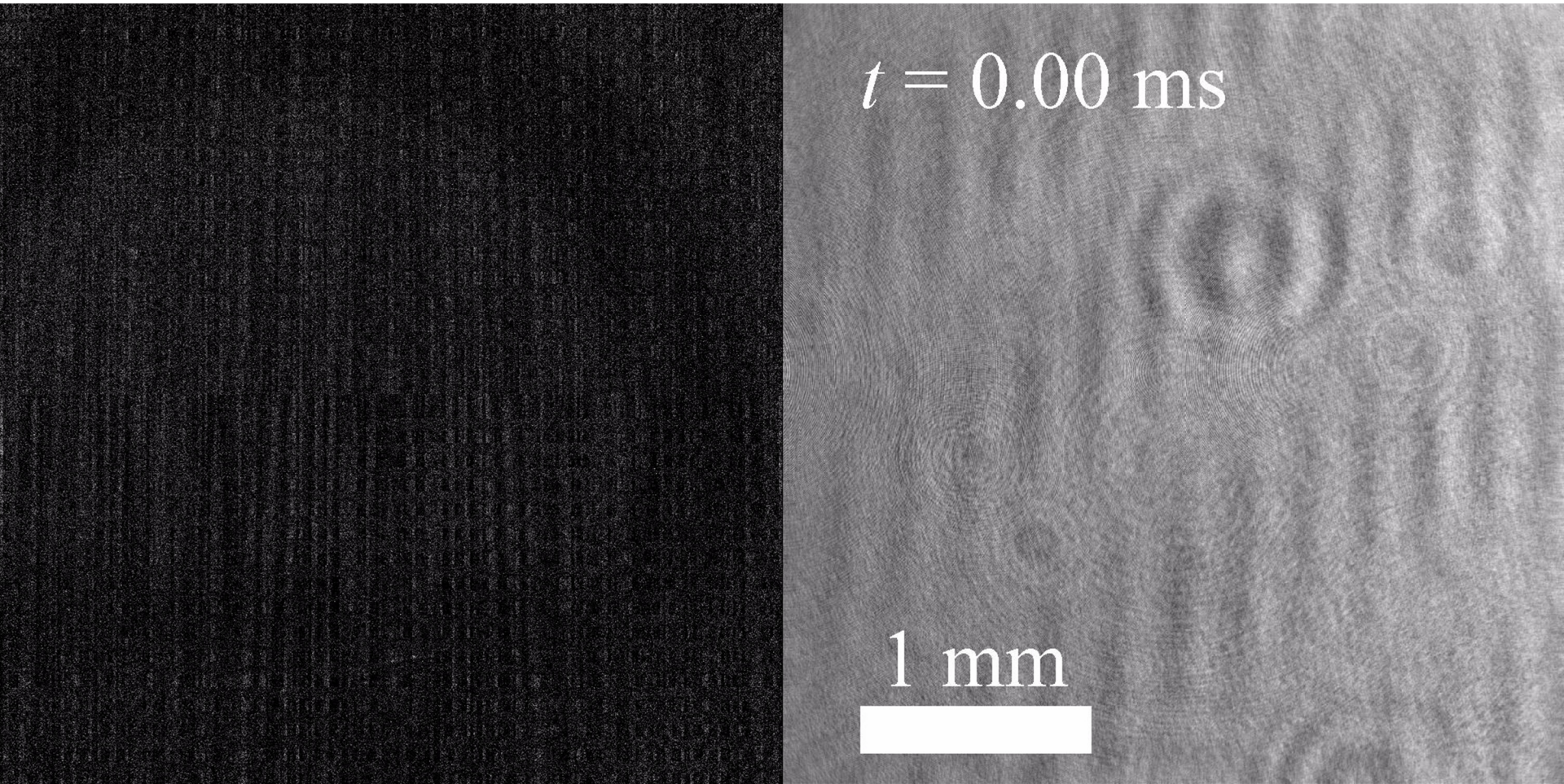
- Beam quality is sufficient for DIH
- Freezes high-speed particles and penetrates through flash and smoke
- Noise due to soot and index-of-refraction gradients

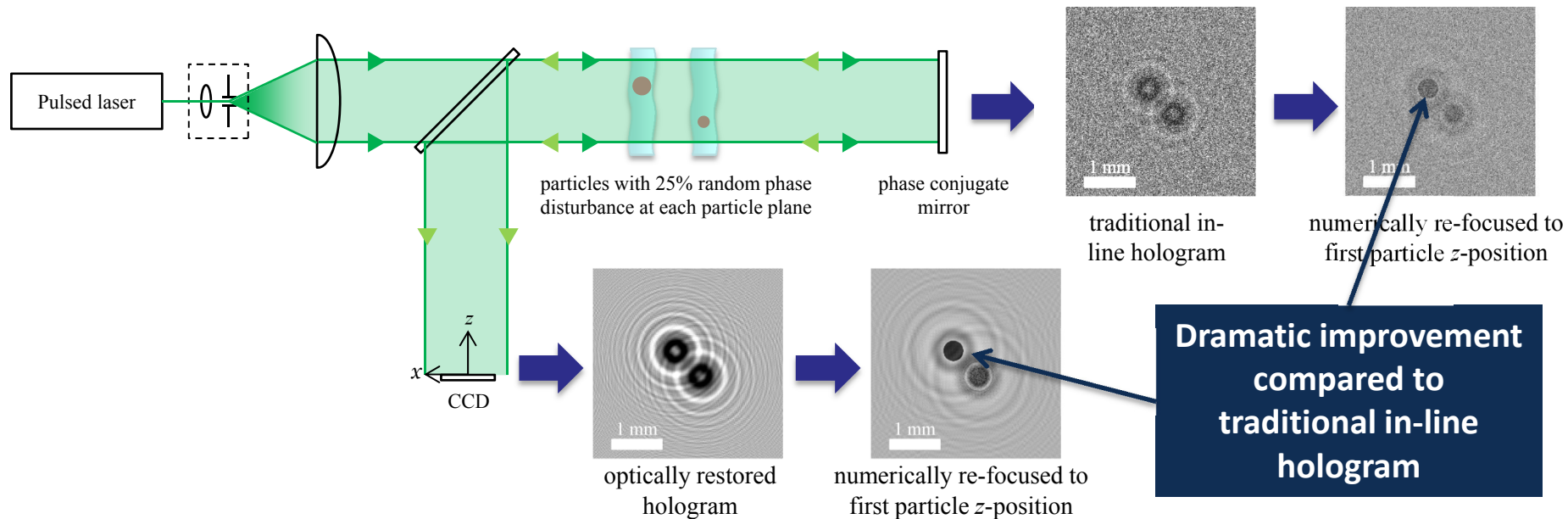# Optical challenges in DIH

Coherent imaging is susceptible to:

- Image distortion through index of refraction gradients

- Loss of phase in[formation] to multiple-scat[tering]

$z = 0.0$ mm

2 mm

Desired: optical corrections to remove these noise sources before recording
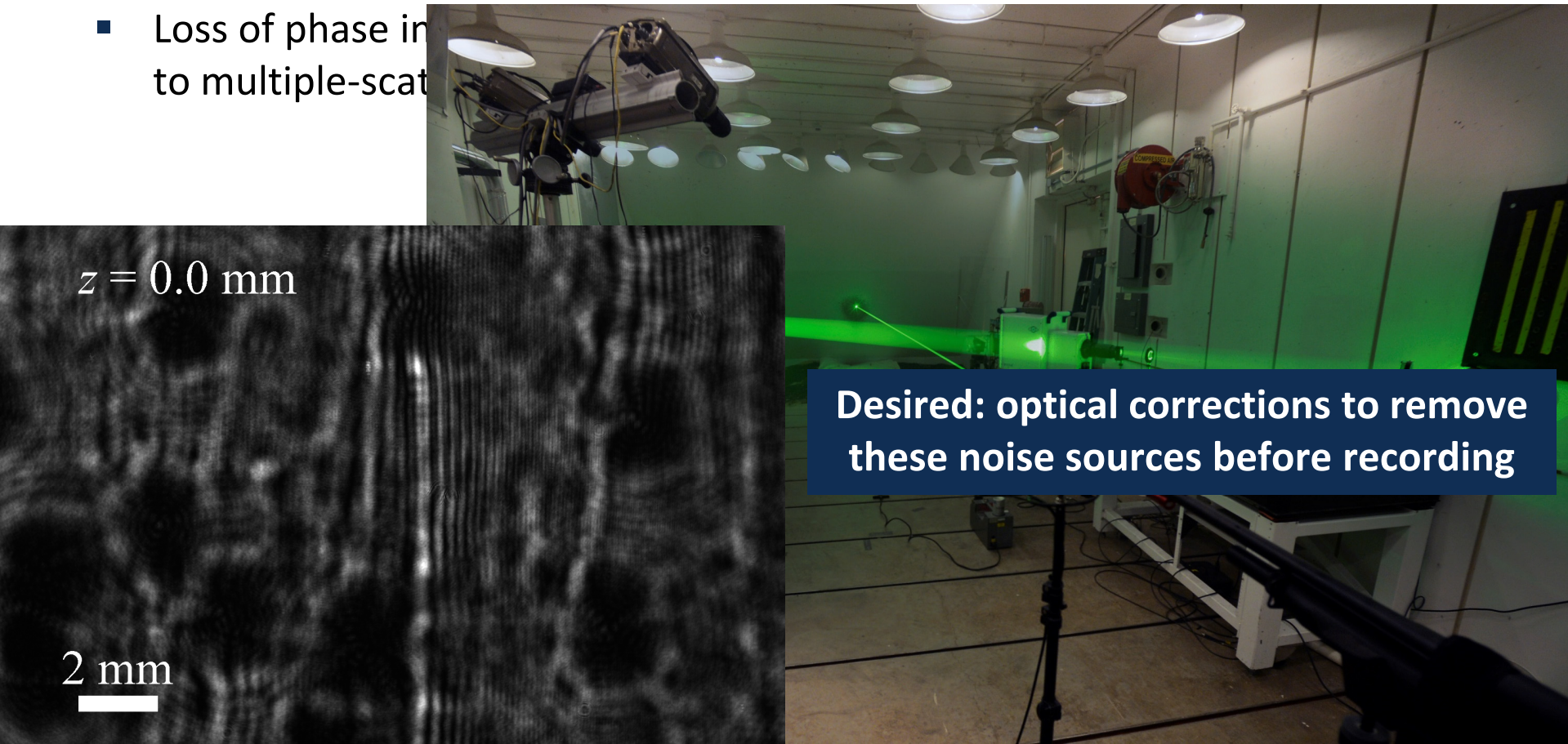
Reconstructed amplitude throughout depth, z Holography configuration for shotgun investigations

Phase-conjugate DIH theory

particles with 25% random phase disturbance at each particle plane

phase conjugate mirror

traditional in-line hologram

numerically re-focused to first particle z-position

optically restored hologram

numerically re-focused to first particle z-position

Dramatic improvement compared to traditional in-line hologram

- Phase-conjugate mirror reflects the incoming wave with opposite phase
  - Non-linear optical effect achieved through passive means (stimulated Brillouin scattering) or active means (degenerate four-wave mixing)
- After double passing, the phase disturbance is canceled

SBS phase-conjugate DIH

A focused beam in a non-linear medium induces phase conjugation via stimulated Brillouin scattering (SBS)
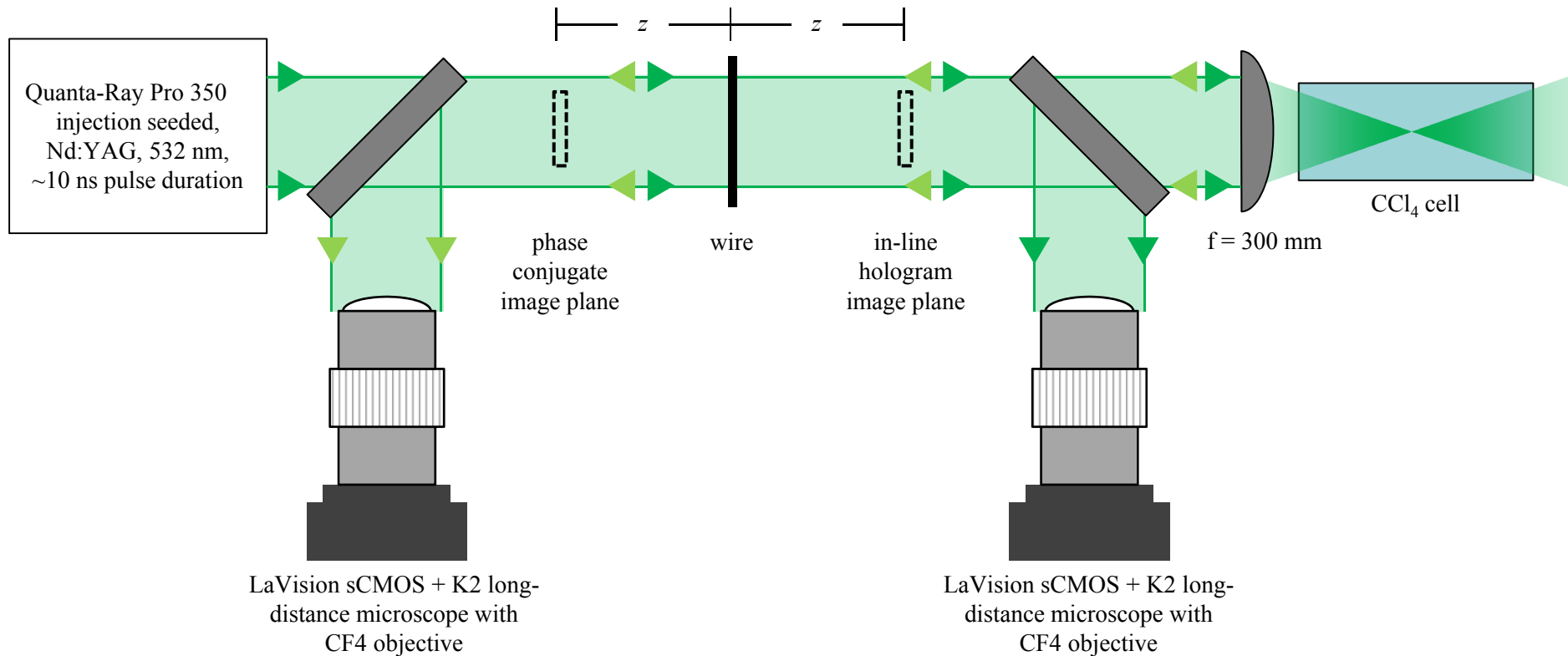
SBS phase-conjugate DIH

Without a disturbance both views give similar results
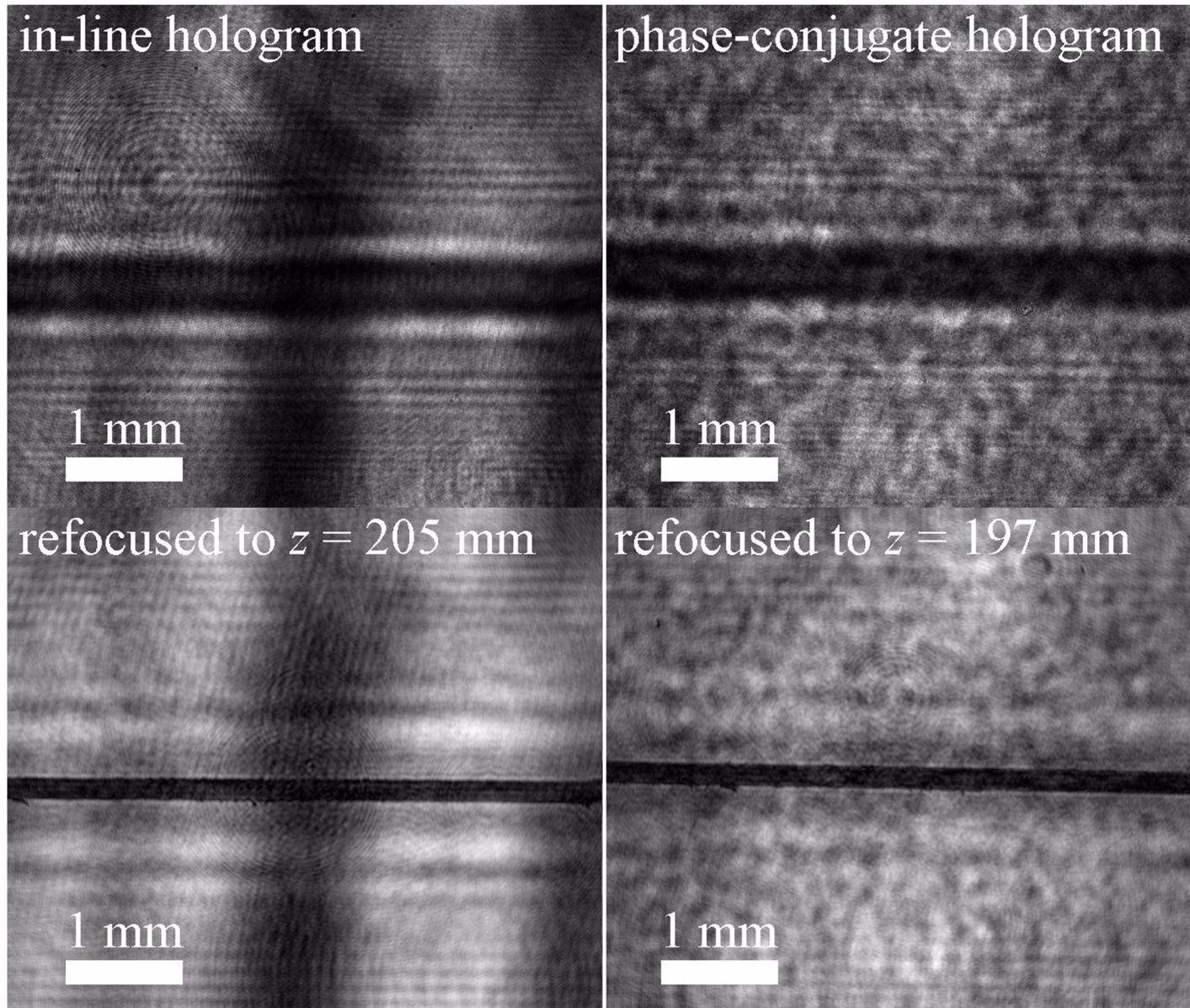
SBS phase-conjugate DIH

A focused beam in a non-linear medium induces phase conjugation via stimulated Brillouin scattering (SBS)

- A misaligned lens in the beam path causes a phase disturbance

Quanta-Ray Pro 350 injection seeded, Nd:YAG, 532 nm, ~10 ns pulse duration

phase conjugate image plane

wire

in-line hologram image plane

$f = 300$ mm

CCl_4 cell

phase disturbance ($f = 2000$ mm)

LaVision sCMOS + K2 long-distance microscope with CF4 objective

LaVision sCMOS + K2 long-distance microscope with CF4 objective
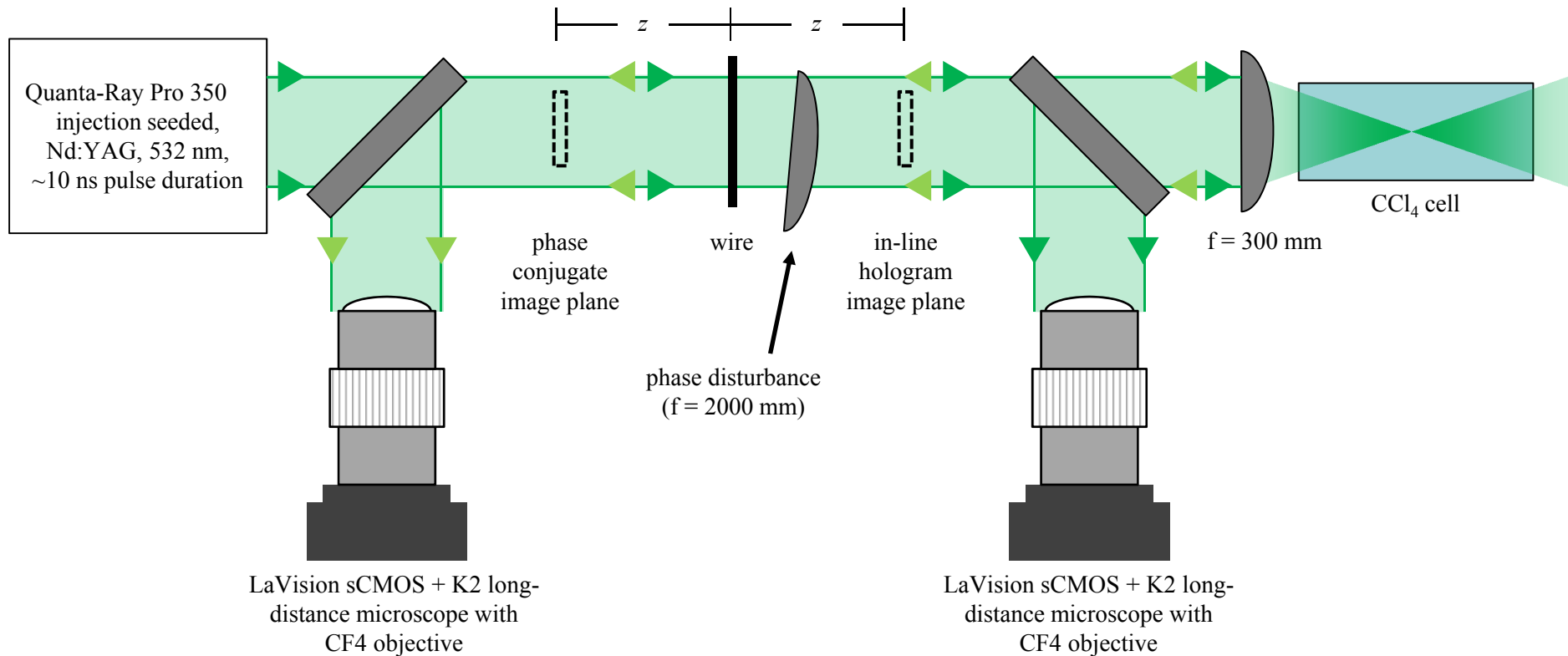
SBS phase-conjugate DIH

Phase conjugation corrects image distortion
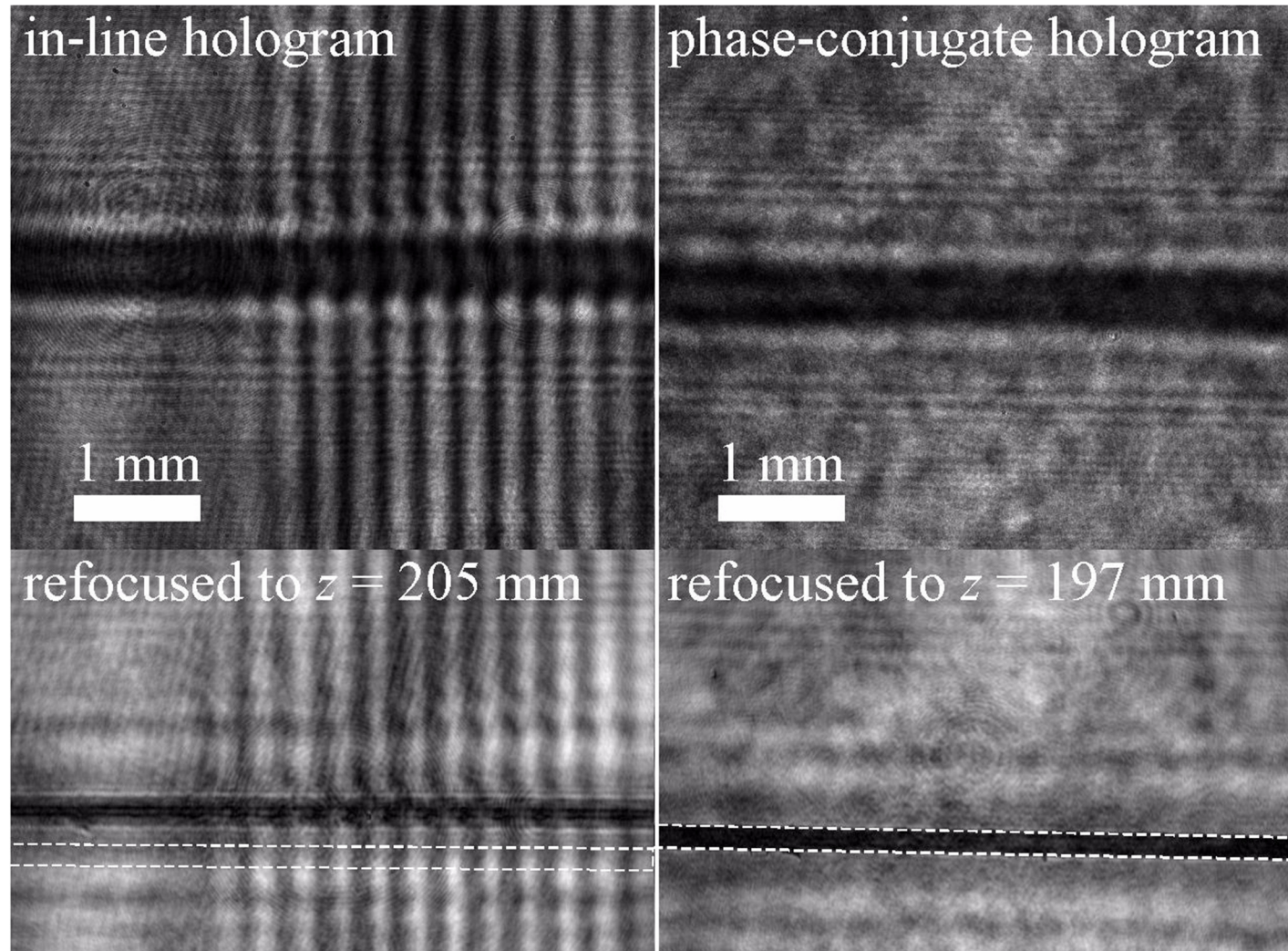
See poster: *Phase conjugate digital inline holography (PC-DIH)* by Kathryn Hoffmeister, Sean Kearney, and Daniel Guildenbecher

Ballistic DIH

Multiple scattering can be reduced through ps time gating

- Combination with DIH might enable scatter free 3D imaging through optically dense media

  - First proposed by: Trolinger et al 2011, *International Journal of Spray and Combustion Dynamics*
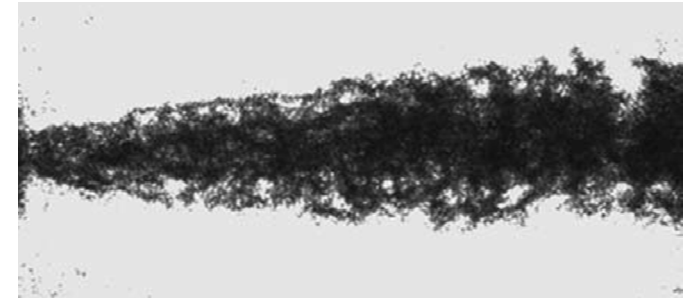
ballistic image of a diesel spray
(Linne et al 2006, *Exp. Fluids*)

measured gate transmission
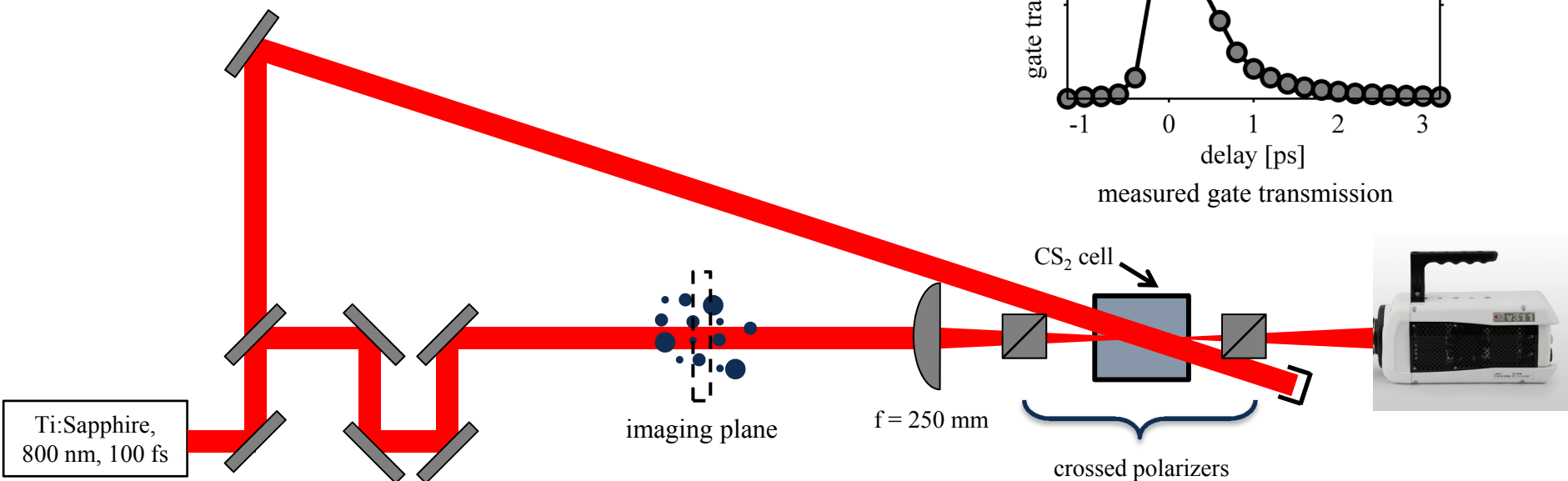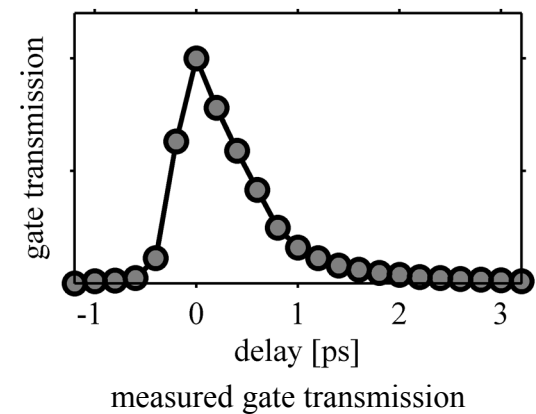
Ballistic DIH

DIH imaging through a Kerr gate (no scatter sources)
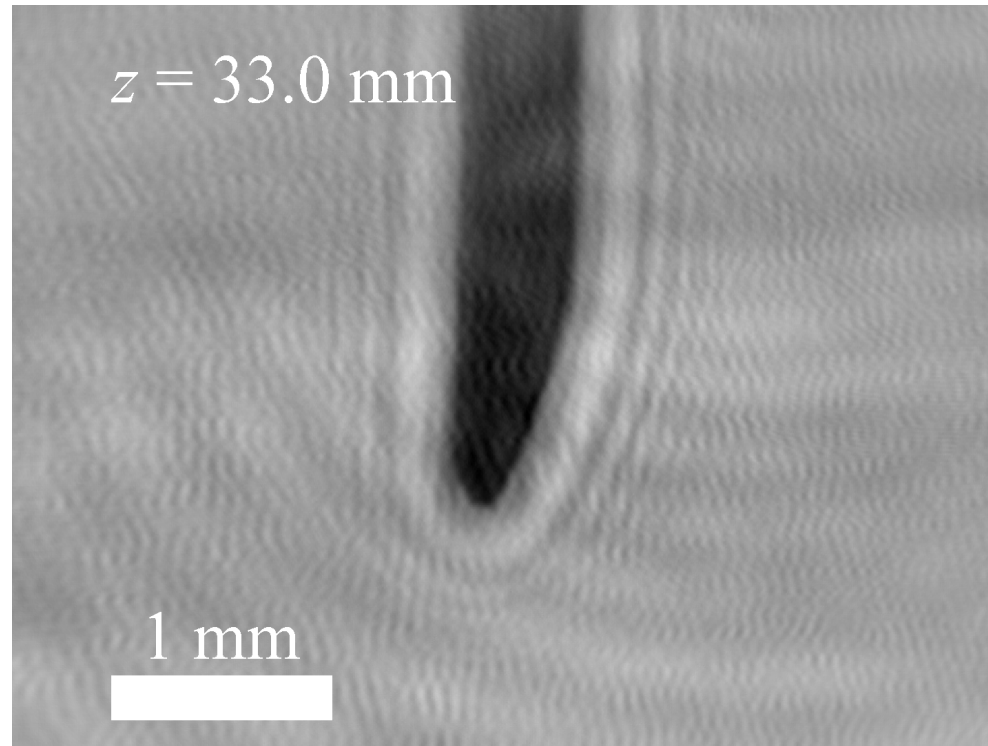
DIH image of a needle recorded with the ballistic configuration (1.6 ps switch delay)

<u>Next step:</u> Explore ballistic DIH through dense scattering sources

- Challenge: *Are there sufficient ballistic photons to form a coherent image?*

Conclusions

DIH has many advantages:	… and opportunities for research:
• 3D-3C measurement	• Depth-of-focus problem
• Rapid quantification of statistics	• Data processing
• Simple optical configuration	• Optical improvements

Acknowledgements:

Questions

Backup slides

Where is the reference wave?

spatial filter   collimating optics   particle field   CCD
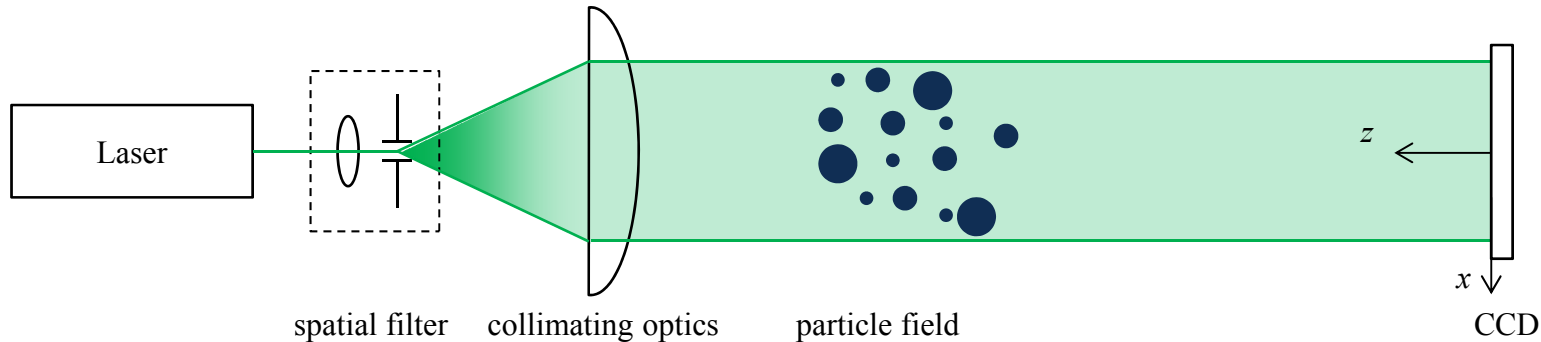
Hologram is the combination of object and reference waves: $h = |E_o+E_r|^2$

- Reconstruction with E_r gives: $h \cdot E_r = (|E_o|^2 + |E_r|^2)E_r + |E_r|^2 E_o + E_r^2 E_o^*$

  DC term   virtual image   real image

  - In off-axis holography, these terms are spatially separated are we attempt to reconstruct the original object wave, E_o

- In in-line holography, we actually want to reconstruct the combination of the reference wave and object wave, E_o+E_r

  - Rearranging: $h \cdot E_r = |E_o|^2 E_r + |E_r|^2(E_o+E_r) + E_r^2 E_o^*$

    DC term   virtual image   real image

SBS phase-conjugate DIH

A hot plate creates a phase disturbance in the air
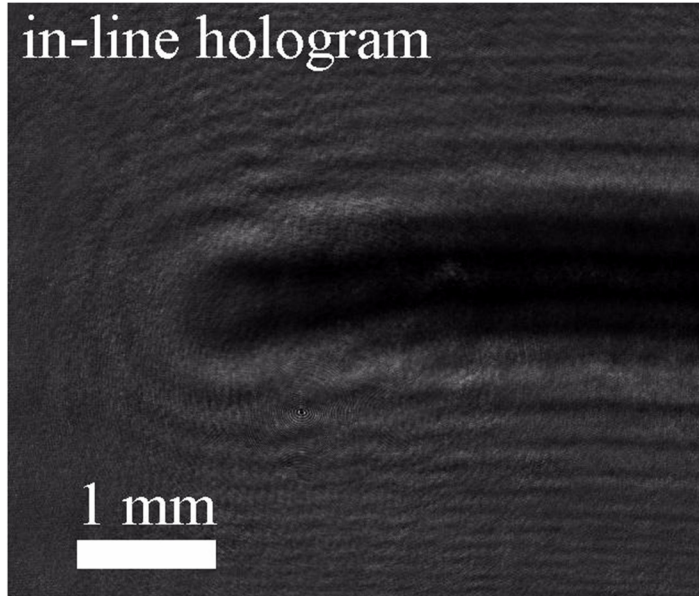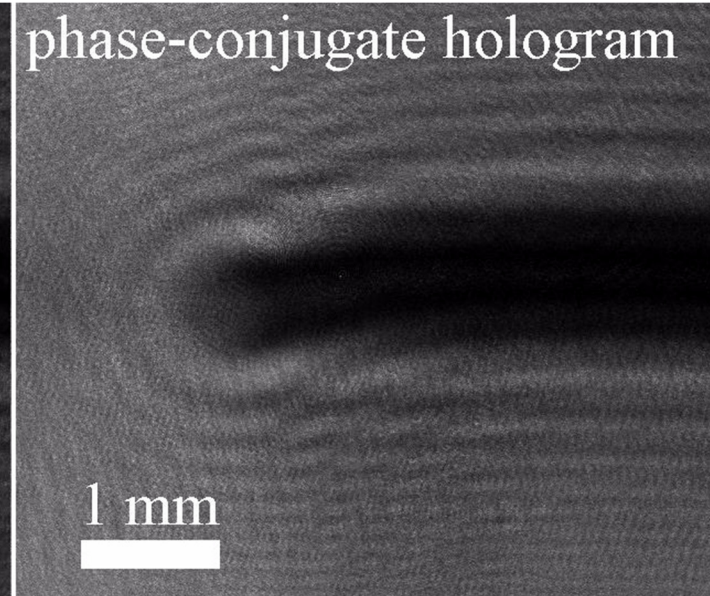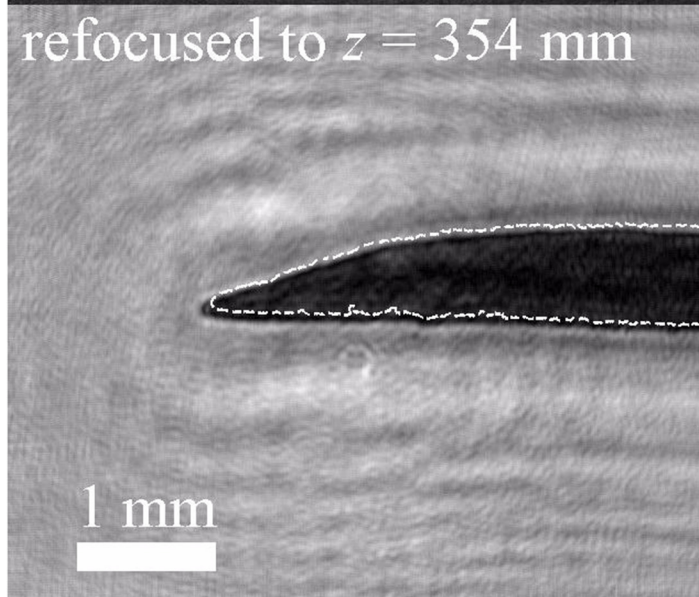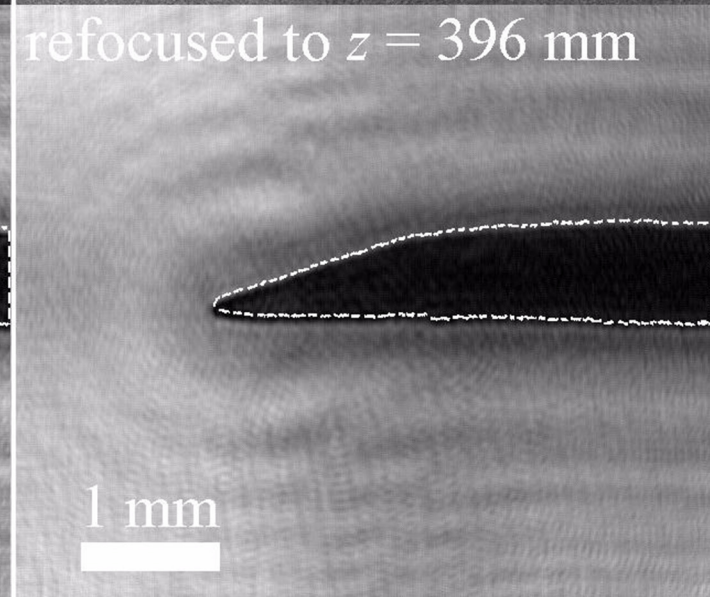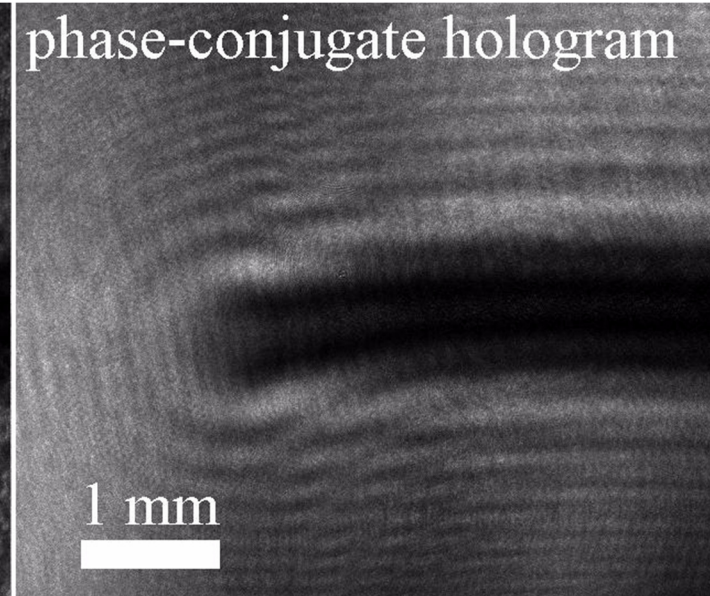
SBS phase-conjugate DIH

A butane igniter creates a more severe phase disturbance
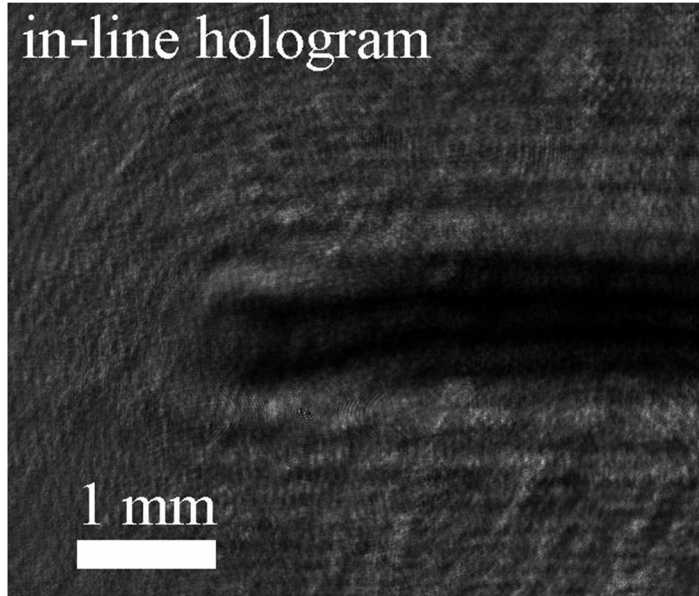
4-wave mixing phase-conjugate DIH

phase
conjugate
virtual CCD

wire

in-line
hologram
virtual CCD

CCl_4 cell

phase disturbance

LaVision sCMOS + K2 long-distance microscope with CF4 objective

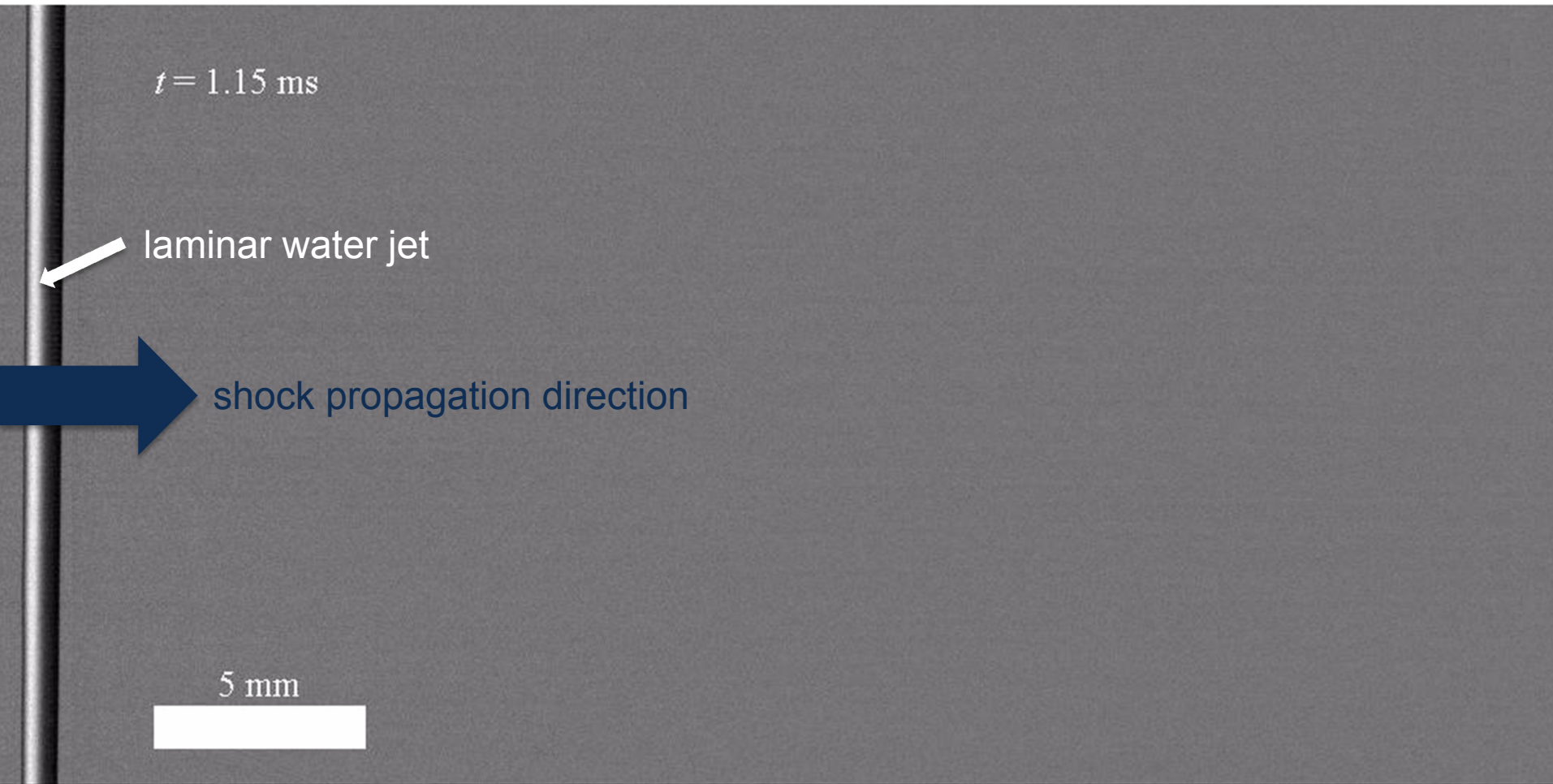LaVision sCMOS + K2 long-distance microscope with CF4 objective
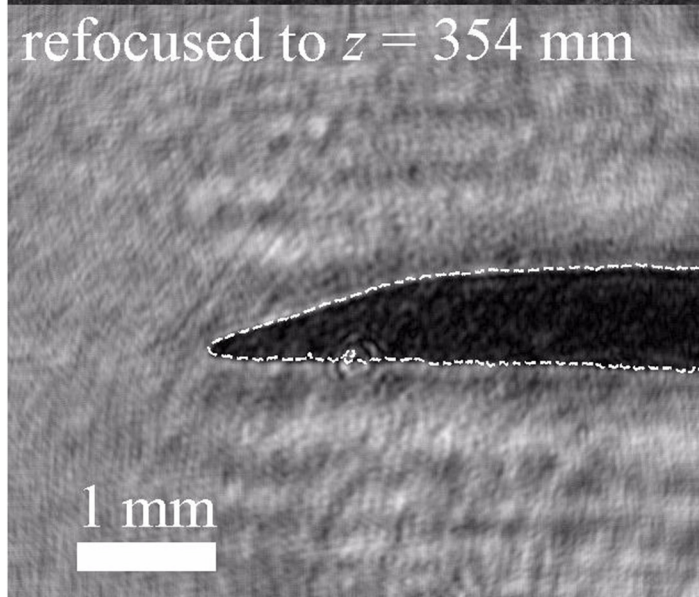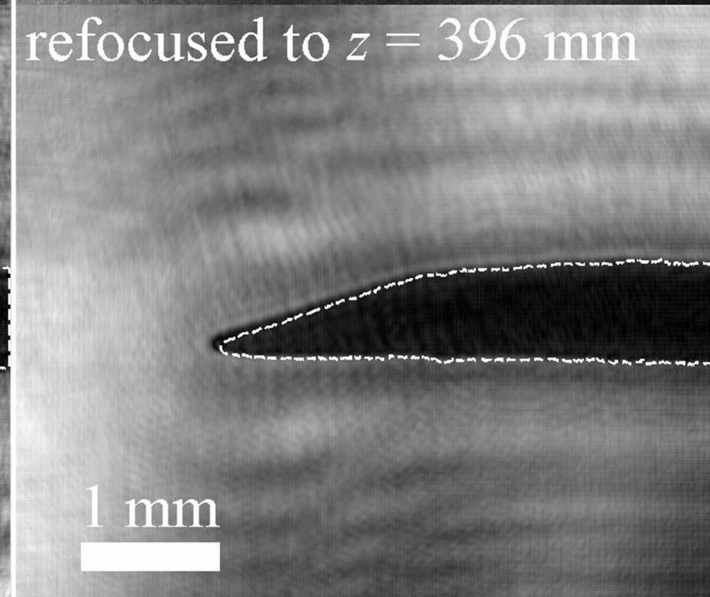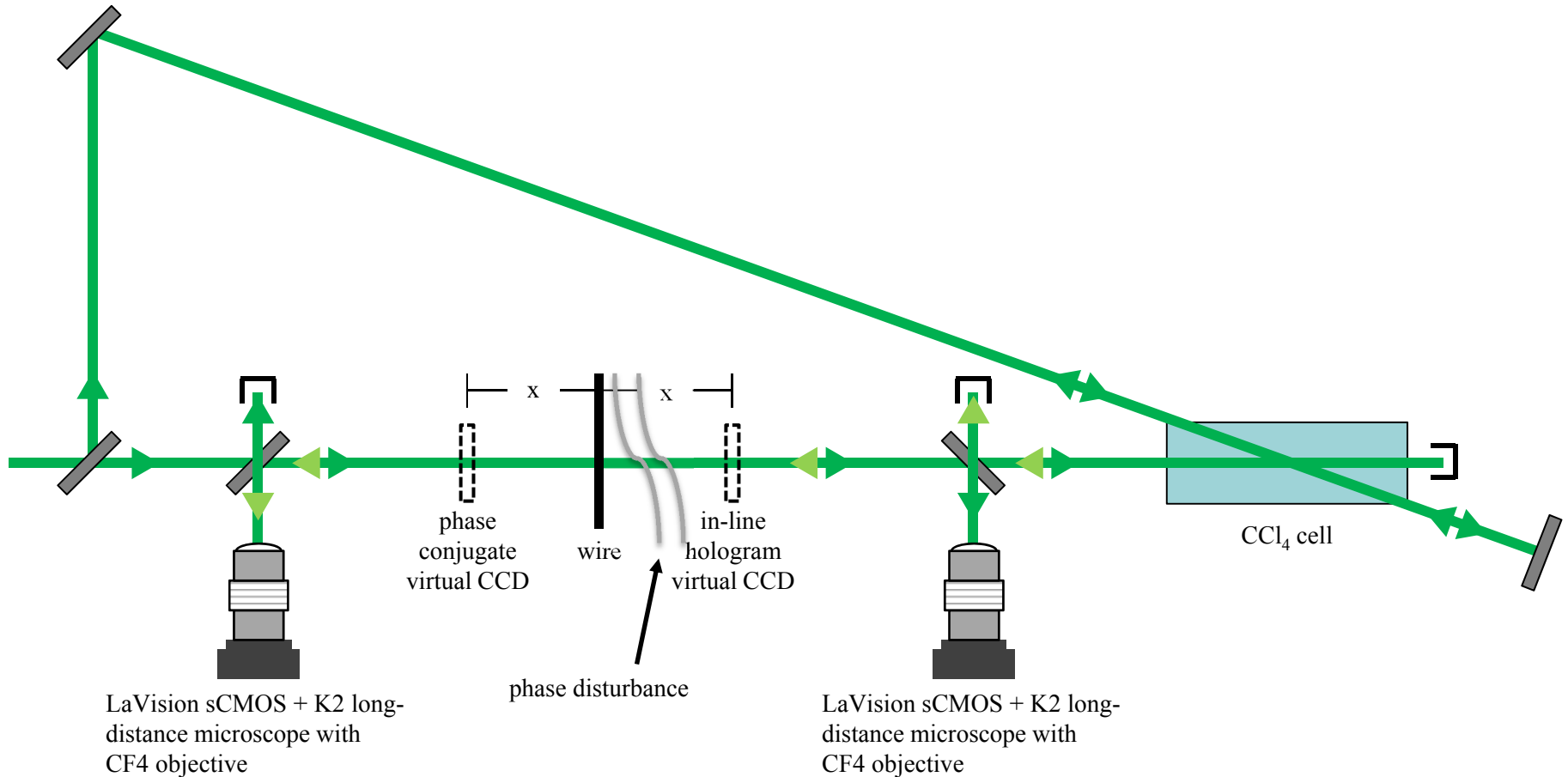
4-wave mixing phase-conjugate DIH

Glass with a uneven layer of optical glue creates a severe distortion

Breakup of a water jet in a shock-tube

$t = 1.15$ ms

laminar water jet

shock propagation direction
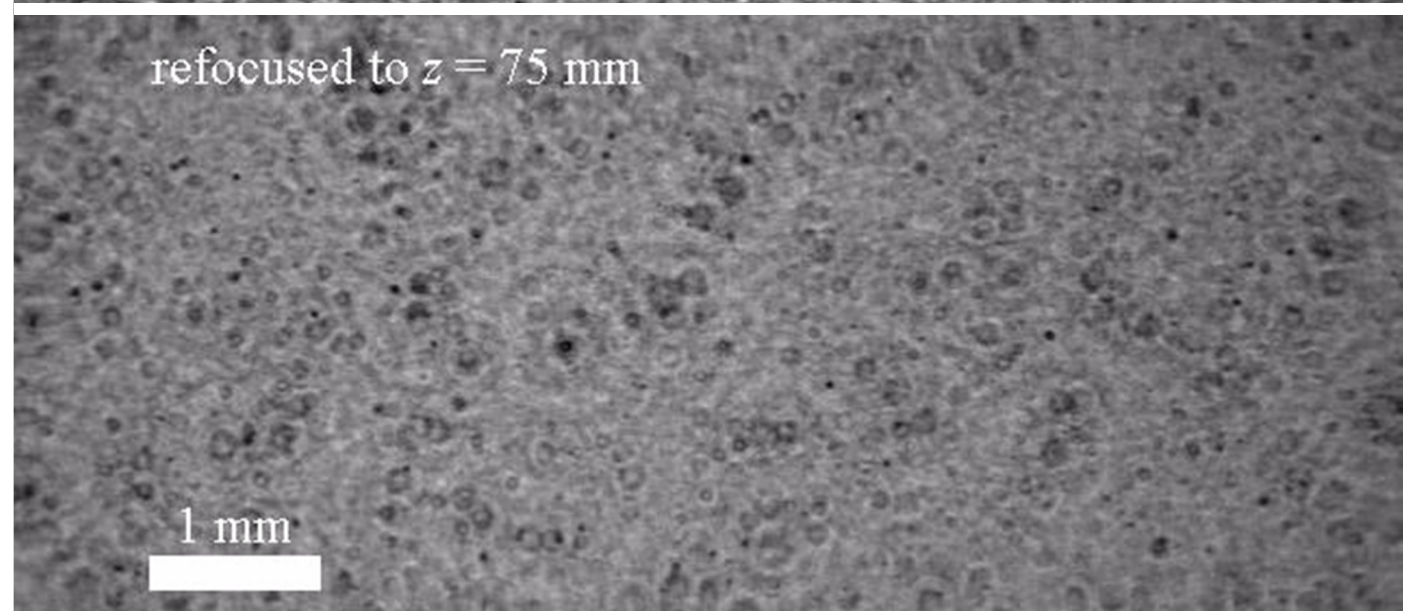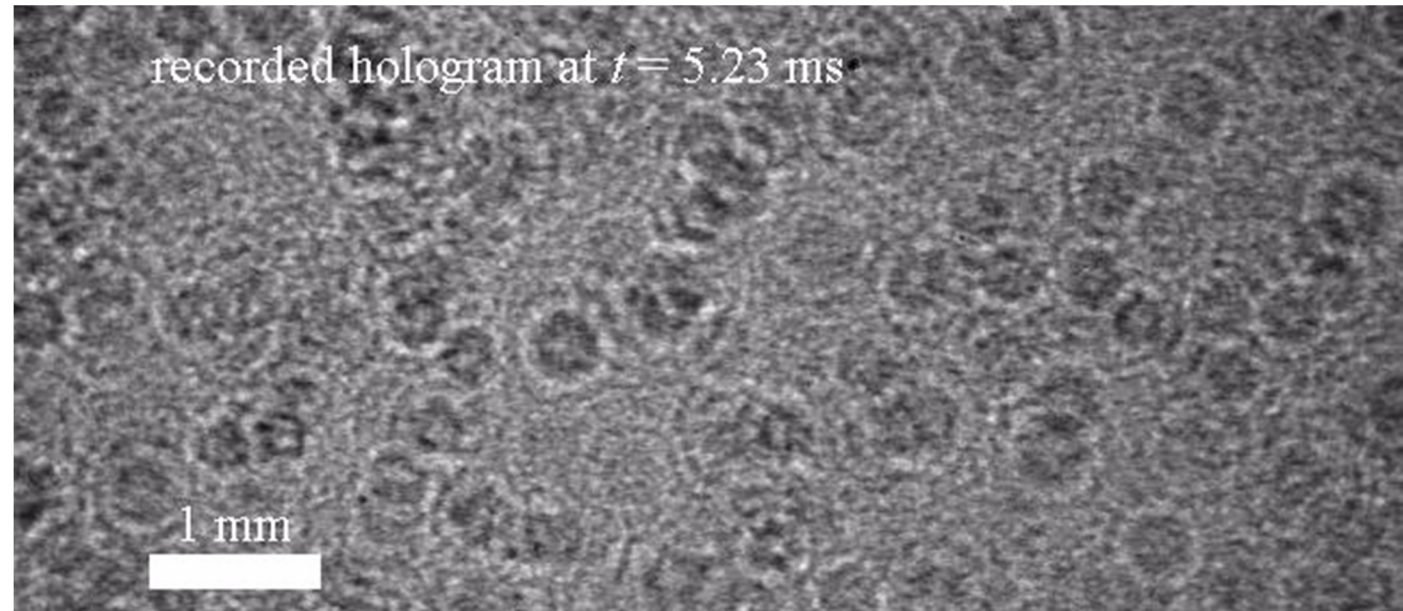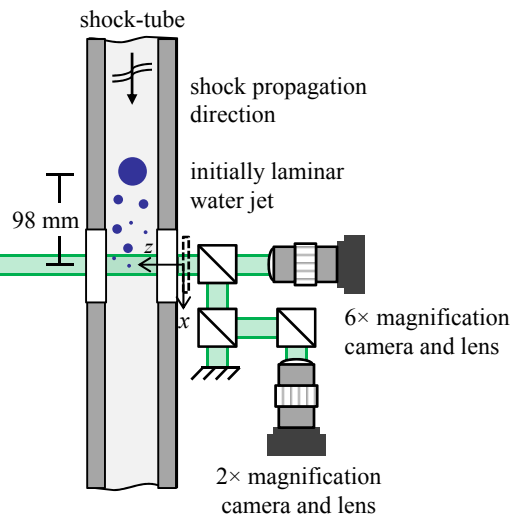
5 mm
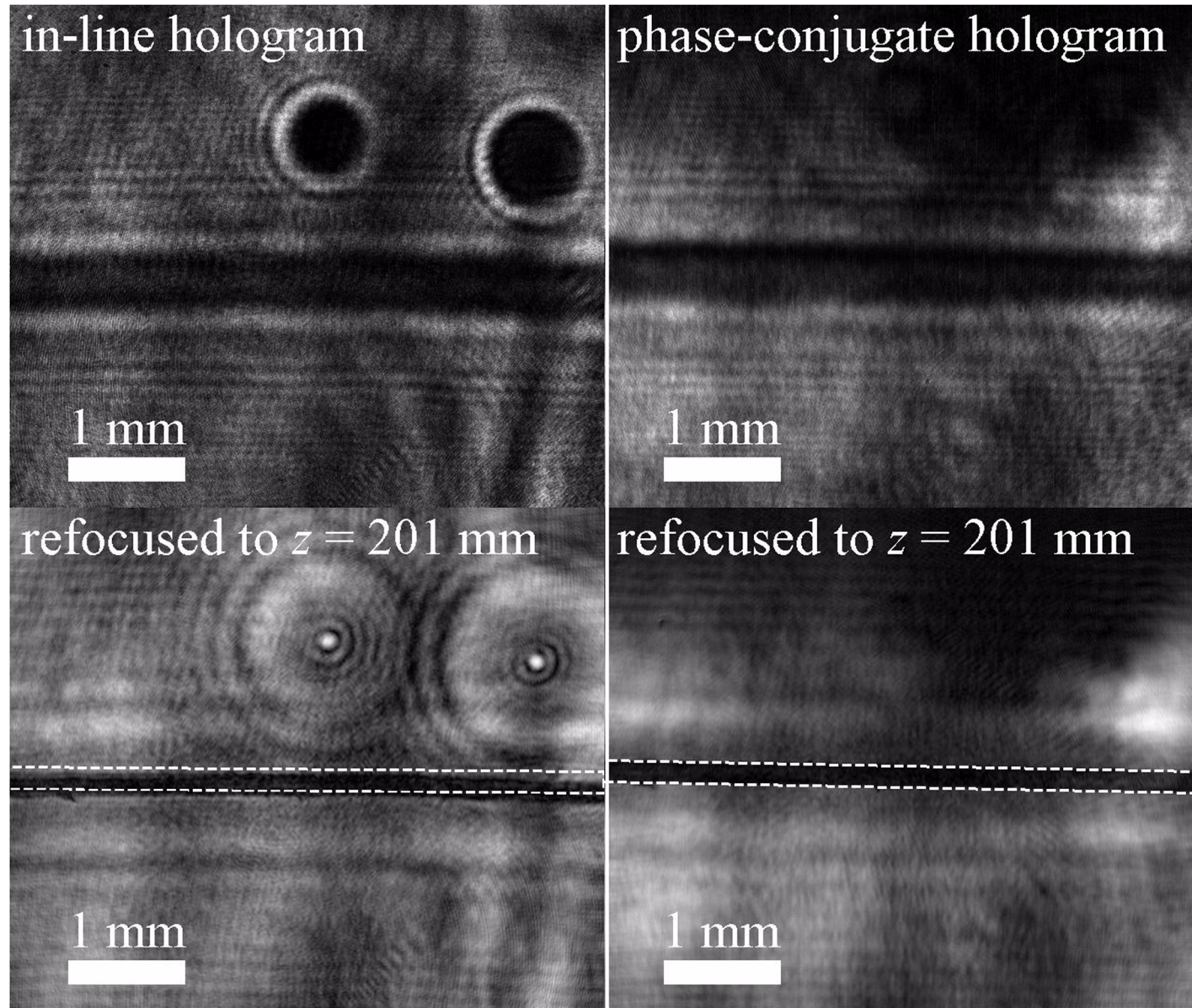
Goals:
1. Quantify the fragment sizes and velocities as a function of shock strength
2. Investigate the relation between surface instabilities and fragment properties

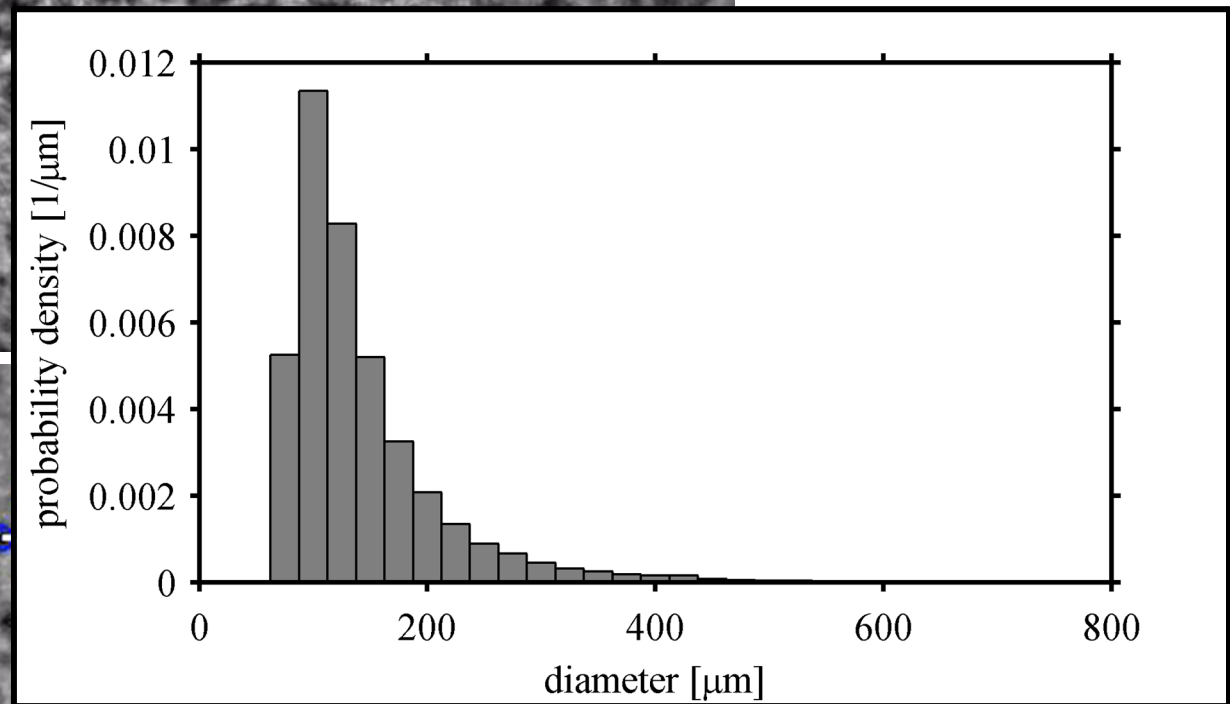# Breakup of a water jet in a shock-tube

Breakup of a water jet in a shock-tube

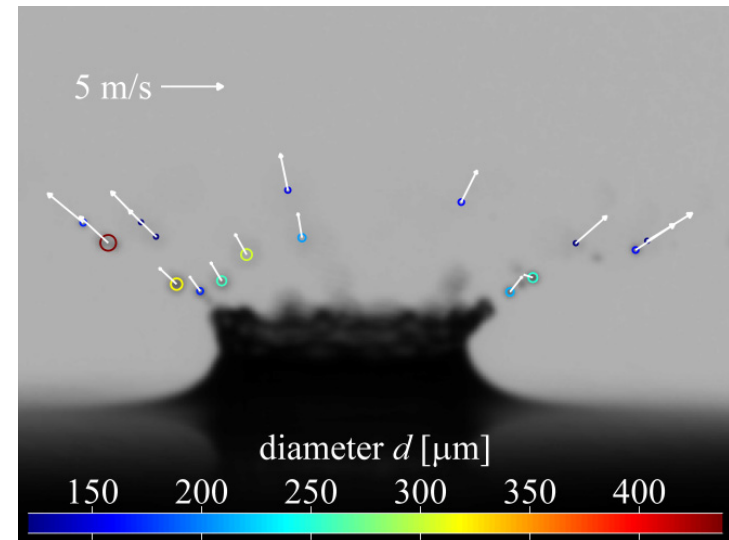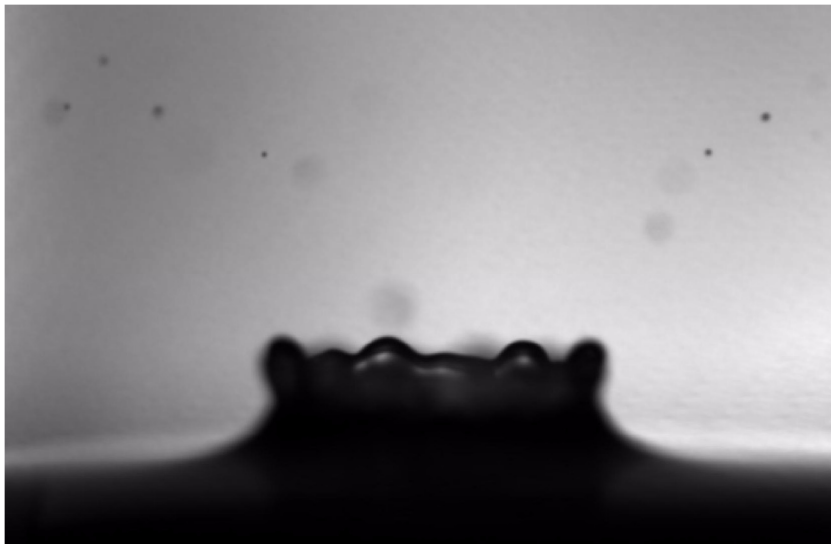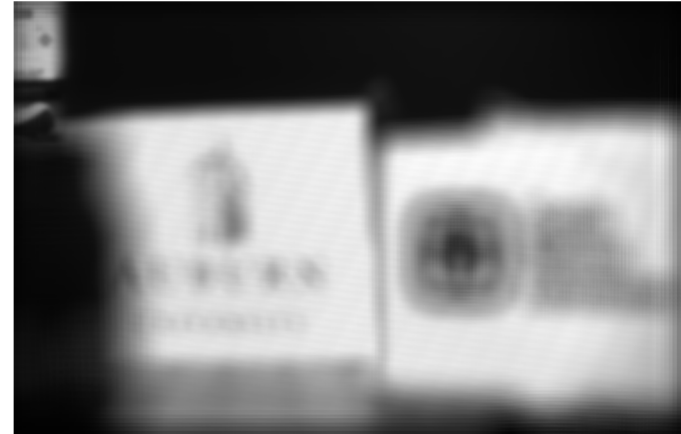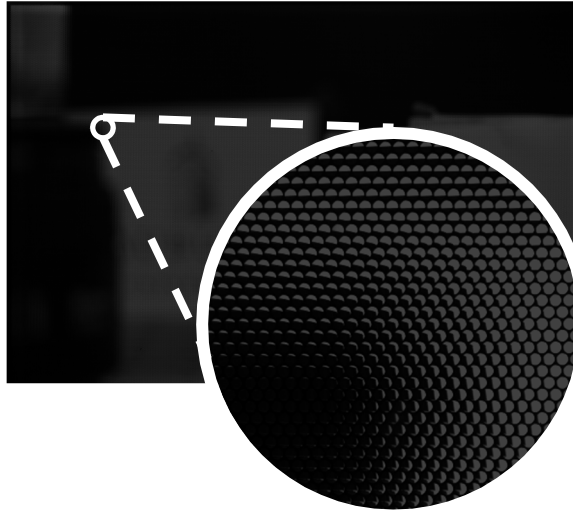recorded hologram at $t = 6.81$ ms

1 mm

70 m/s

1 mm

Alternative 3D measurements

Plenoptic cameras use micro-lens arrays and white light to create a 3D image
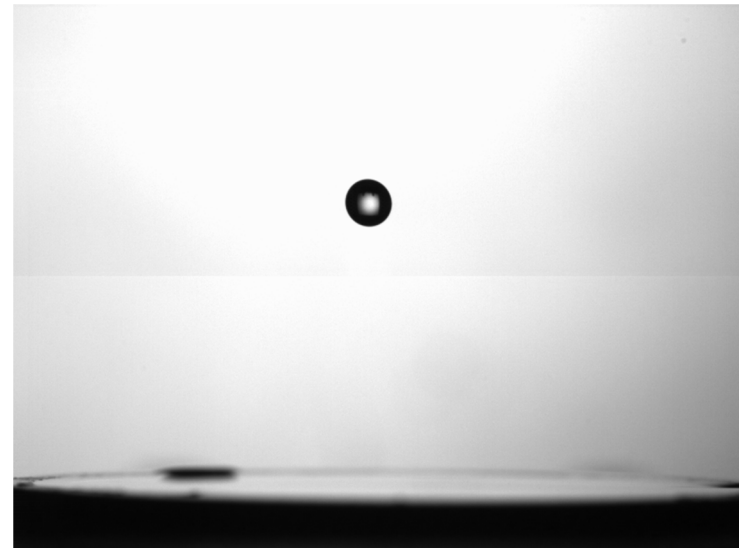
Drop impact on a thin film

Motivation: measurement of secondary droplets by other methods requires significant experimental repetition
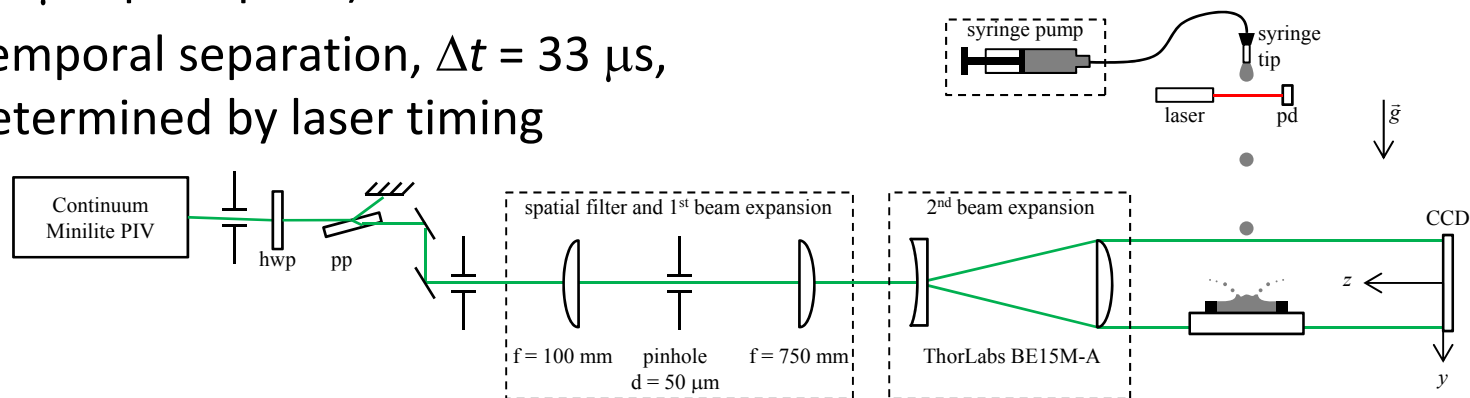
- Process symmetry provides opportunities to validate accuracy

Experimental configuration:

- Double pulsed laser (λ = 532 nm, 5 ns pulsewidth)

- Interline transfer CCD (4872 × 3248, 7.4 μm pixel pitch)

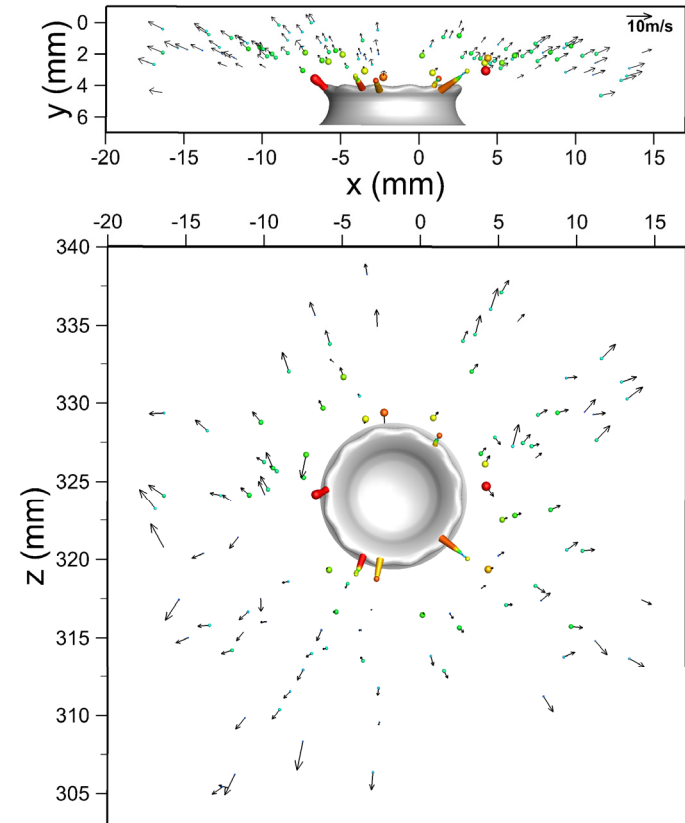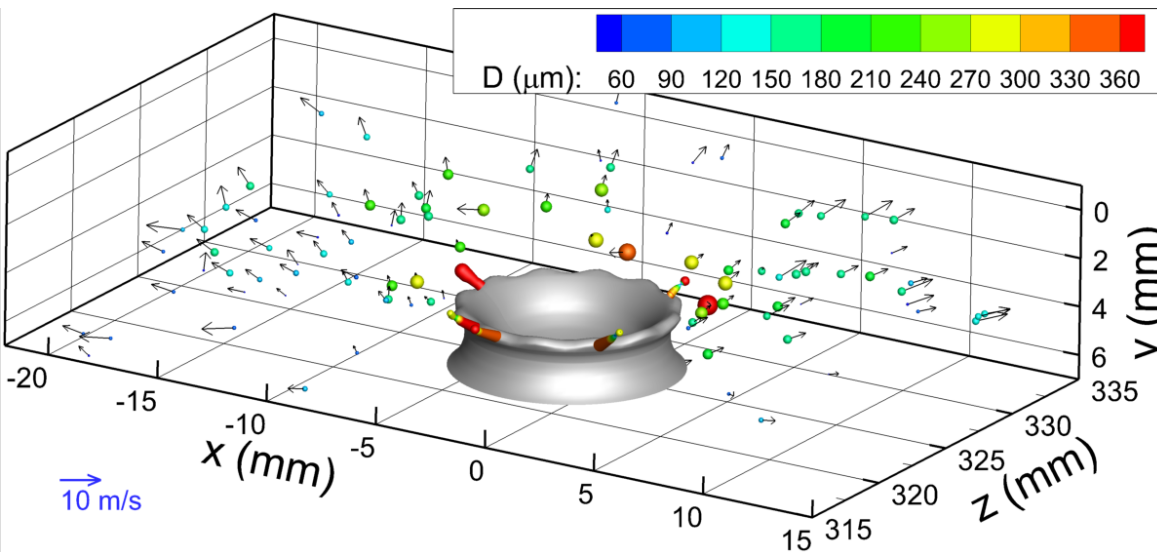- Temporal separation, Δt = 33 μs, determined by laser timing
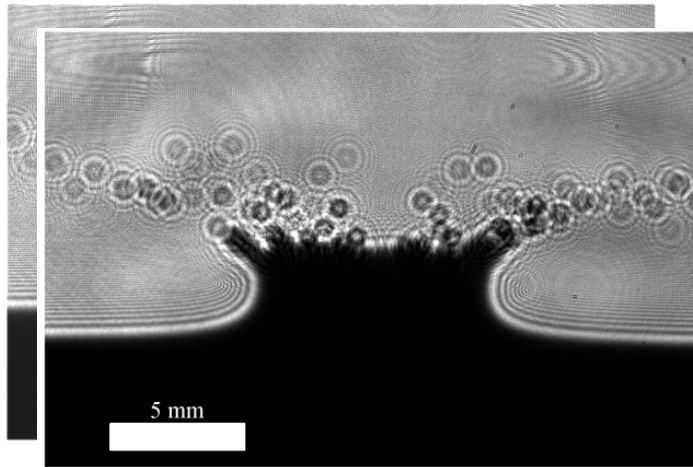

impact of a 3 mm water drop on a 2 mm water film
(Guildenbecher et al, 2013, *Exp. Fluids*.)

experimental configuration of holographic recording of drop impact on a thin film
(Guildenbecher et al, 2014, *Exp. Fluids*.)

# Drop impact on a thin film

Processed with the hybrid method

holographic reconstruction of
drop impact on a thin film
(Guildenbecher et al, 2014, *Exp. Fluids*.)

Percussion primers

Motivation: No viable technique currently exists to quantify the size and velocity distribution from the hot particles in percussion primers

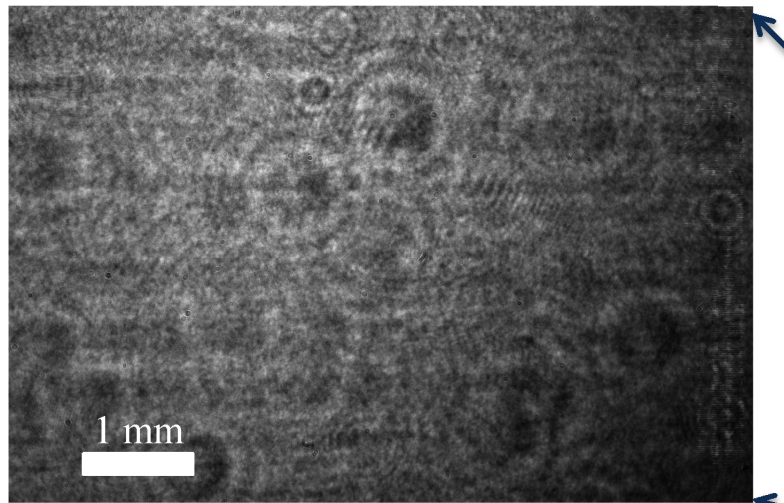Experimental configuration:

- Double pulsed laser (λ = 532 nm, 5 ns pulsewidth)

- Interline transfer CCD (4872 × 3248, 7.4 μm pixel pitch)

- ~6X magnification achieved using Infinity K2 long distance microscope with CF-4 objective

- Temporal separation, Δt = 2 μs, determined by laser timing
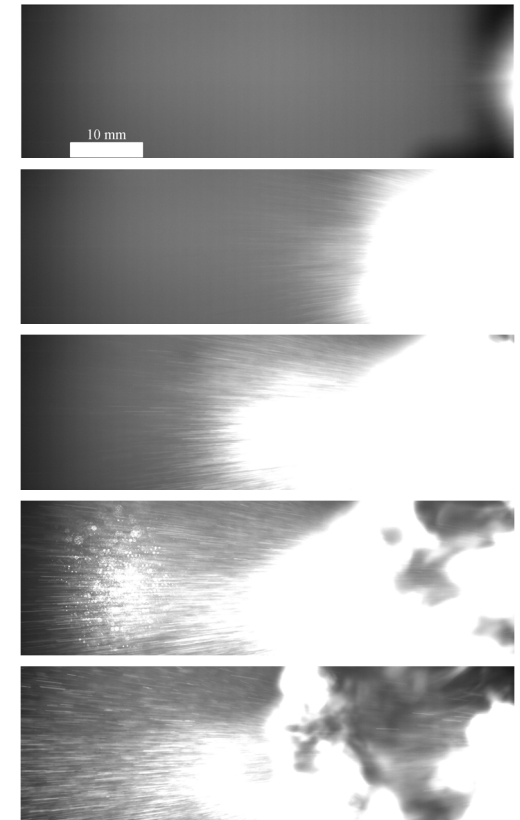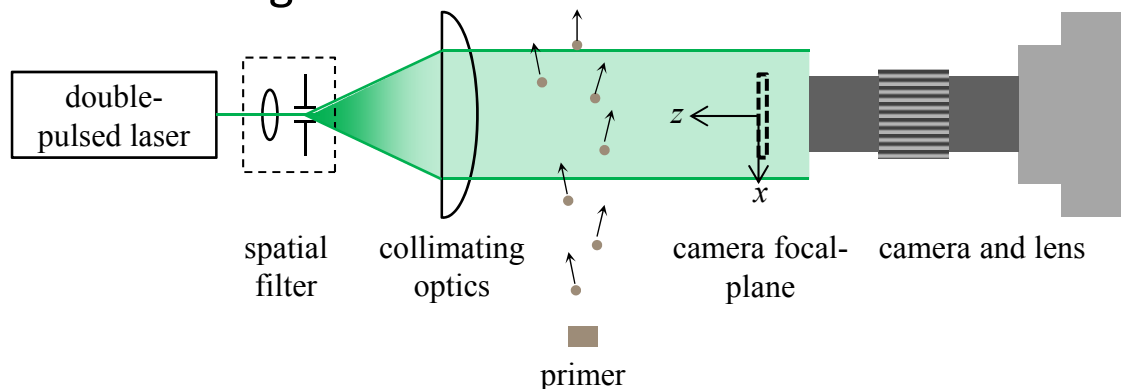
High-speed video of event

Percussion primers

Five holograms recorded at these conditions

Recorded hologram

First known quantification of particle size

- Particle size distribution shows the expected behavior
- Probability goes to zero at large and small particle diameters
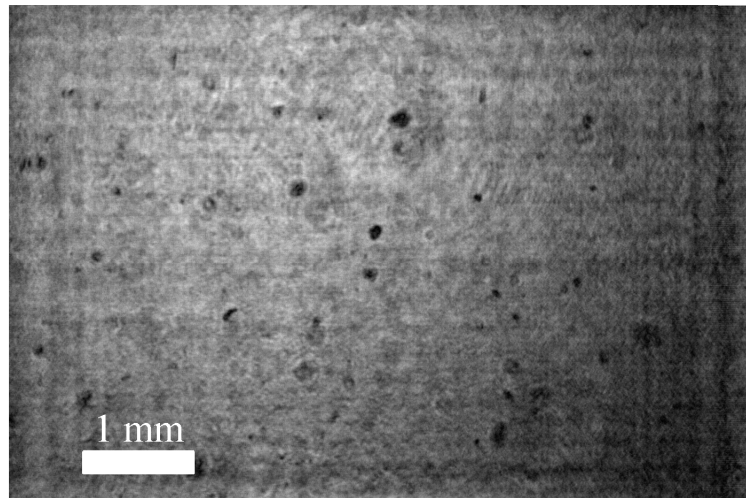
Numerically re-focused to $z = 200$ mm from the CCD

Cross-correlation method

Theory: in-focus particle images from two sequential holograms contain correlated information

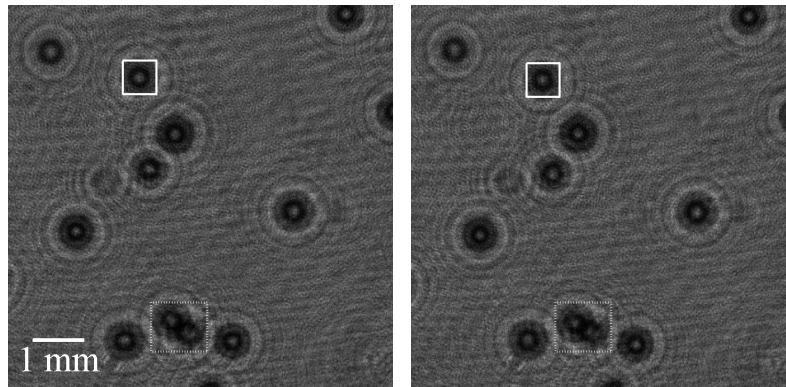- The maximum cross-correlation, c, gives the displacement (Δx, Δy)
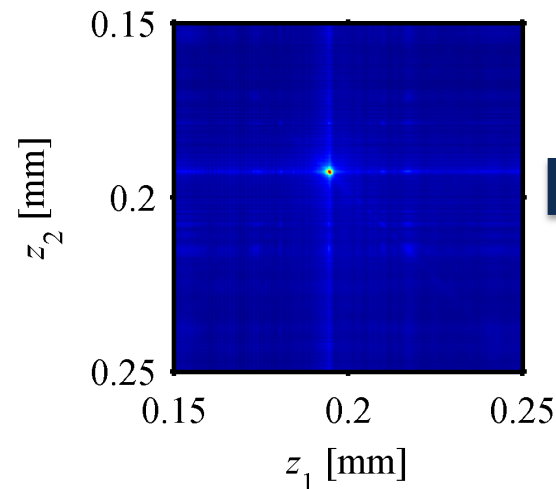
$$c = \max_{\Delta x, \Delta y} \left[\sum_m \sum_n \text{Img}_1(m,n) \text{Img}_2^*(m,n)(m-\Delta x, n-\Delta y) \right]$$

- Img_1 and Img_2 chosen as the edge sharpness images from the two frames

- z positions in each frame (z_1 and z_2) are found from the maximum value of c over all possible combinations of z_1 and z_2

1 mm

hologram
(Guildenbecher et al,
2013, *Opt. Lett.*)

hologram after displacing
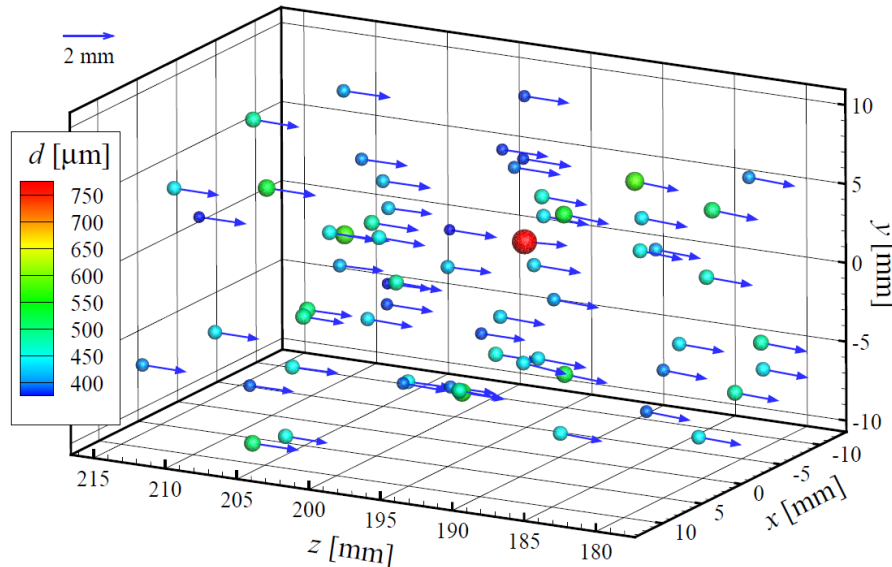the particle field by 2 mm
(Guildenbecher et al,
2013, *Opt. Lett.*)

maximum value of c for the particle in the white
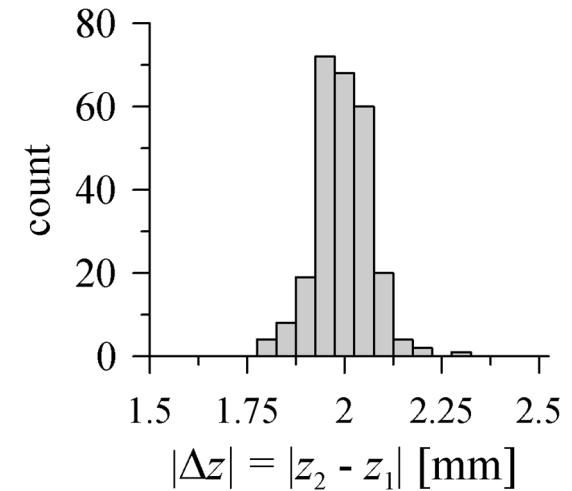boxes (Guildenbecher et al, 2013, *Opt. Lett.*)

z_1 = 194.72 mm,
z_2 = 192.72 mm,
Δz = 2.00 mm

Cross-correlation method

Again, experimentally validated with quasi-stationary particles in silicone oil

measured displacement field from one realization
(Guildenbecher et al, 2013, *Opt. Lett.*)

measured z-displacements from all realizations
(Guildenbecher et al, 2013, *Opt. Lett.*)

- Actual displacement = 2.0 mm

- Mean detected displacement = 1.996 mm +/- 0.072 mm

  - Standard deviation of 0.15 times mean diameter

  - Order of magnitude improvement compared to uncertainties in the literature
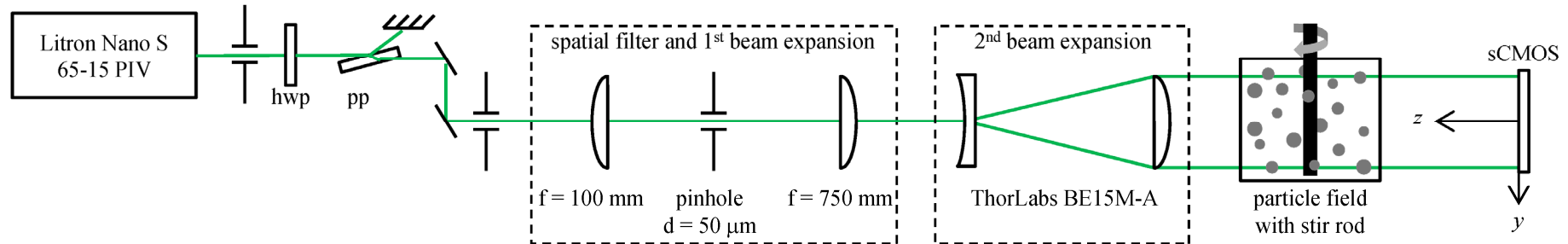
Sonic pellets from a shotgun
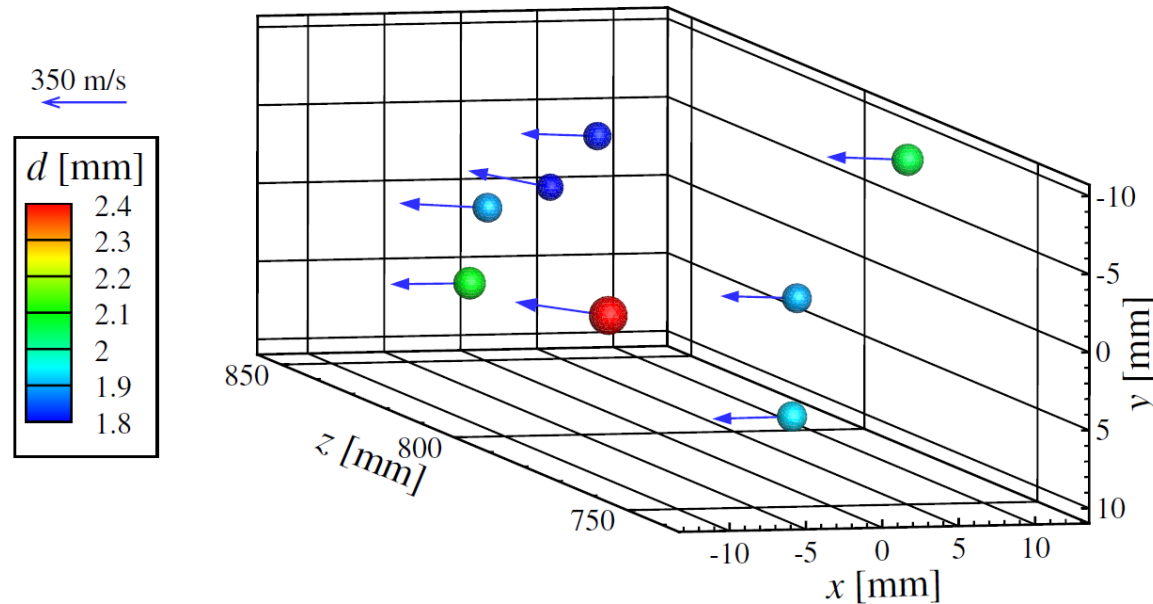
particle field from the shotgun measured with the cross-correlation method
(Guildenbecher et al, 2013, *Opt. Lett.*)

Results closely match the expected mean velocity (350 m/s) and diameter (2.0 mm)

- Uncertainty in Δz is on the order of 0.2 particle diameters

3D, 3C fluid velocity measurements?

- Particles stirred by a rotating rod (r_0 = 1.58 mm, ω_0 = 100 rpm)

- Recorded at 15Hz with a LaVision sCMOS camera (2560 × 2160, 6.5 μm pixel pitch)
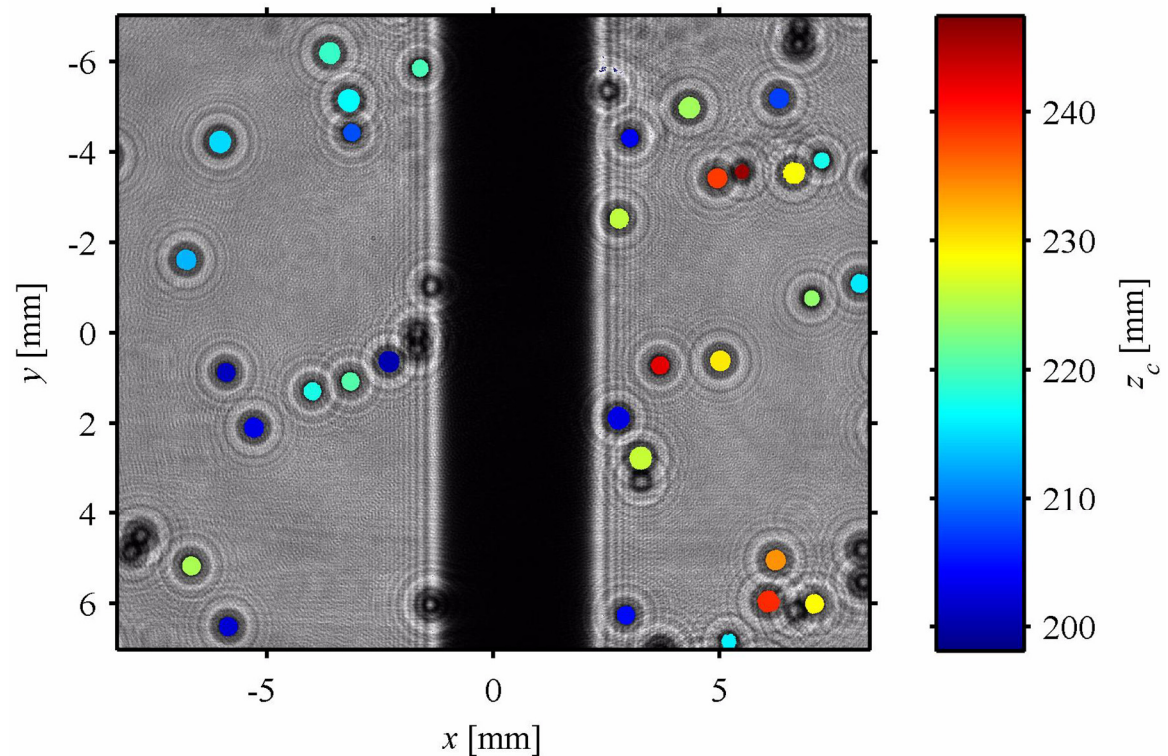
particles measured with the hybrid method, background shows the recorded holograms

3D, 3C fluid velocity measurements?
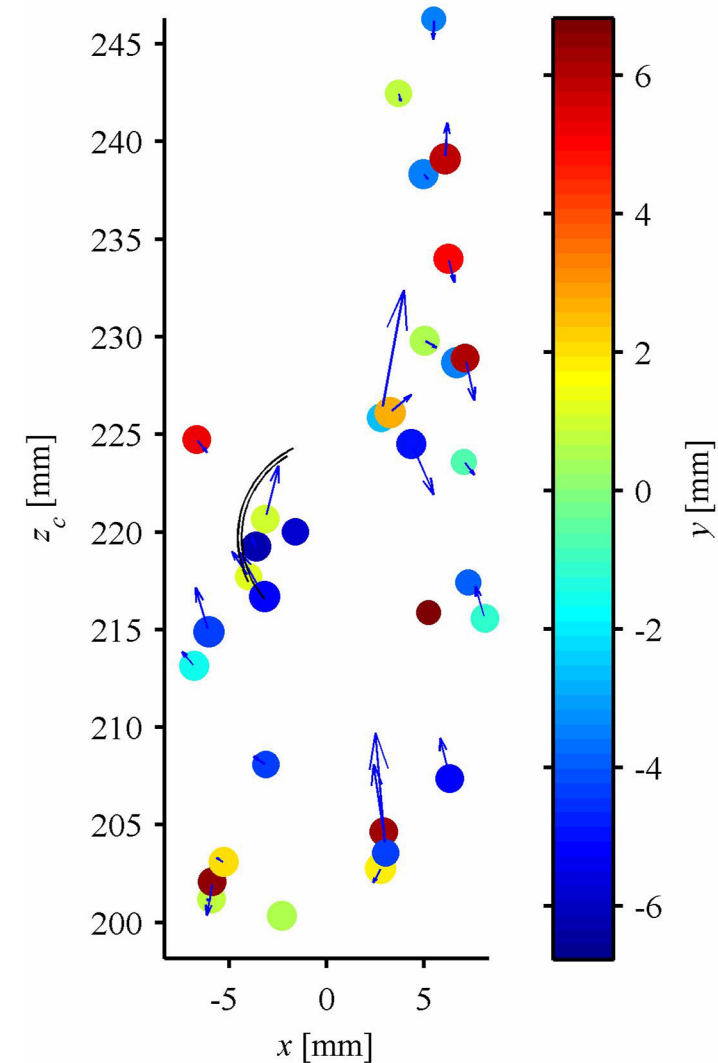
For all trajectories

- Error in measured z = -0.04 $\pm$ 1.51 mm
- Error in measured Δz = -0.03 $\pm$ 1.05 mm
  - Standard deviation of $2.3 \cdot \bar{d}$

Experiments repeated with smaller particles ($\bar{d} = 118 \mu m$, see paper for details)

- Error in measured z = -0.003 $\pm$ 0.379 mm
- Error in measured Δz = -0.001 $\pm$ 0.302 mm
  - Standard deviation of $2.6 \cdot \bar{d}$

Next steps:

- Compare results with alternative particle detection methods
- Use results to quantify effects of particle overlap and other experimental noise sources

all measured x-z trajectories vs. predicted

3D, 3C fluid velocity measurements?

Advantages:

- Simple optical setup requiring only one line-of-sight view

- Large depth of field (hundreds of mm possible)

- Particle sizes can be measured (if desired)

Challenges:

- High uncertainty in the z-direction

- Particle field must be relatively sparse providing only limited vectors

- Vectors at random positions

- Methods not as mature as PIV or even tomographic-PIV

Note: the literature contains many works on holographic-PIV. My own work has not been focused on these applications

mean measured x-z velocities